UNIVERSITY OF TURKU

Spatial Lipidomics of Lesioned Mouse Striatum: Modelling Neuroinflammatory Mechanisms in MS

Neurometabolic Lab Turku

Master's thesis

MDP in Human Neuroscience

Author:

Silke Jansma

08.09.2025

Turku

The originality of this thesis has been checked in accordance with the University of Turku quality assurance system using the Turnitin Originality Check service. Turnitin Similarity score is 15%.

Subject: Master's thesis MDP in Human Neuroscience
Author: Silke Jansma
Title: Spatial Lipidomics of Lesioned Mouse Striatum: Modelling Neuroinflammatory Mechanisms in Multiple Sclerosis
Supervisors: Alex Dickens & Daniel Anthony
Number of pages: 68 pages
Date: 08.09.2025

Abstract

This thesis investigates changes in lipid composition in the mouse striatum following the induction of multiple sclerosis-like neuroinflammatory lesions. Using Mass Spectrometry Imaging (MSI) supported by hypothesis testing and Principal Component Analysis (PCA), spatial lipid alterations were assessed within and across hemispheres in lesion and sham-control animals. Lesion-associated lipid signatures included increases of ceramides, phosphatidylcholines (PCs), and phosphatidylethanolamines (PEs), consistent with inflammatory activation, membrane remodelling, and neurodegeneration. These changes were most apparent when comparing the lesioned striata to the sham control striata with hypothesis testing. PCA further identified lipid species that, while not always statistically significant in isolation, contributed strongly to overall variance, suggesting coordinated biochemical responses to injury. The inclusion of broad anatomical regions may have introduced noise and obscured some of the lesion-specific lipid changes. Despite these limitations, the study demonstrates the utility of spatial lipidomics for detecting subtle, region-specific metabolic disruptions in models of neuroinflammation. These results suggest that MSI-based lipid profiling holds promise for identifying biomarkers and provides mechanistic insights into neuroinflammation and multiple sclerosis.

Keywords: Neuroinflammation, Multiple Sclerosis, Lipidomics, Mass-Spectrometry Imaging, MS-lesion Study, Neurodegenerative Disorder.

.

Table of contents

1 Introduction

The brain is one of the most lipid-rich organs, with lipids making up nearly half of its dry weight (Podbielska et al., 2021). These lipids are essential for membrane structure, energy storage, and cell signalling (Del Boccio et al., 2011). Lipid metabolism is disrupted in neurodegenerative diseases like multiple sclerosis (MS) (Ferreira et al., 2020). MS involves chronic inflammation that attacks the brain's myelin, leading to impaired nerve function (Ferreira et al., 2020). Lesion formation in MS triggers biological processes like blood-brain barrier breakdown, immune cell infiltration, and glial activation (Ferreira et al., 2020). Lipids play a central role in these processes, influencing repair or aggravating damage through oxidative stress and apoptosis (cell death) (Razo et al., 2024). Most research on neuroinflammation has focused on protein and gene expression changes following brain injury (Hansen & Wang, 2023). However, lipidomic alterations in MS remain underexplored, especially in specific brain regions (Oliveira-Lima et al., 2018). Traditional lipidomic approaches often average data across large areas, missing important localised changes at the injury site (Oliveira-Lima et al., 2018). A deeper understanding of lipid responses in these regions could provide new insights into inflammation, injury, and injury repair mechanisms (Oliveira-Lima et al., 2018).

Mass spectrometry imaging (MSI) offers a solution to this challenge. MSI allows for the detailed mapping of lipid distributions in tissue, providing spatial resolution that reveals local metabolic changes (Oliveira-Lima et al., 2018). Applying traditional statistical methods to MSI data reveals concrete, significant differences between experimental categories. However, a tool like principal component analysis (PCA) is used to analyse more subtle patterns in complex data (Oliveira-Lima et al., 2018). Overall, MSI visualizes individual lipid distributions, offering obviously distinct differences between lesioned and non-lesioned areas (Oliveira-Lima et al., 2018).

This thesis investigates lipid alterations in the mouse striatum following experimentally induced MS-like lesions using stereotactic surgery. By combining MSI with PCA, the study aims to uncover region-specific lipid changes linked to neuroinflammation. The broader goal is to improve the understanding of lipid disruptions in MS pathology, which could eventually guide the search for new biomarkers and therapeutic strategies to limit damage caused by chronic inflammation (Razo et al., 2024).

2 Theoretical background topic

2.1 Mechanisms of Neuroinflammation

2.1.1 Neuroinflammation

Neuroinflammation refers to the inflammatory response within the brain or spinal cord and represents a distinct physiological process compared to inflammation in other tissues. In general, inflammation is a protective mechanism activated in response to tissue injury or infection, promoting healing and defending the body against harmful stimuli (Razo et al., 2024). While this process is typically acute and beneficial, unresolved inflammation can become chronic and pathological, contributing to disease development in both the central nervous system (CNS) and peripheral organs (Hansen & Wang, 2023). In the CNS specifically, the nature of inflammation is shaped by the brain's immunological specialisation, which differs significantly from the immune response observed in peripheral tissues (Jain et al.,2020; Anthony et al., 2012).

One of the key differences in neuroinflammation is the timing and extent of leukocyte recruitment. Compared to peripheral inflammation, where immune cells are rapidly mobilised to the site of injury, leukocyte infiltration into the injured CNS occurs more slowly (Anthony et al., 2012). This delayed response provides a potential therapeutic window to limit secondary damage. Furthermore, the mediators of inflammation, such as cytokines, chemokines, and lipid-derived molecules, play specialised roles in the CNS, with some acting differently than in peripheral tissues. Despite these differences, systemic cytokine production remains essential for coordinating neuroinflammatory responses, indicating a complex interaction between central and peripheral immune systems (Anthony et al., 2012).

Historically, the brain's relationship with the immune system was viewed from a Cerebro-centric perspective, assuming a largely isolated and autonomous CNS immune environment. However, research by Ransohoff and colleagues redefined this understanding, describing the brain as "immunologically specialised", highlighting its ability to both send and receive immune signals from the periphery (Ransohoff et al., 2003; Anthony et al., 2012). After a brain injury, pro-inflammatory cytokines produced within the CNS can stimulate peripheral immune activation, which in turn leads to the infiltration of immune cells such as leukocytes. These cells assist in repair and debris clearance, but prolonged or excessive inflammation can lead to secondary tissue damage.

Neuroinflammation is also implicated in the pathology of various neurodegenerative diseases, including Alzheimer's disease (AD), Parkinson's disease (PD), multiple sclerosis (MS), and forms of dementia (DiSabato et al., 2016). While chronic neuroinflammation is often harmful, a baseline level of inflammatory signalling, particularly involving cytokines, is essential for maintaining normal brain function. These signals contribute to processes like synaptic pruning, immune surveillance, and memory consolidation (DiSabato et al., 2016). Therefore, understanding the dual roles of neuroinflammation, both protective and damaging, is essential for developing treatments targeting neuroimmune interactions.

2.1.2 Neuroinflammatory cascade

Neuroinflammation is a complicated process that involves various types of cells in the central nervous system (CNS), such as microglia, astrocytes, endothelial cells, and perivascular macrophages (Jain et al., 2020). Microglia, as the primary immune cells in the CNS, constantly monitor immediate surroundings (DiSabato et al., 2016; Jain et al., 2020. When disturbances are detected, microglia become active and release pro-inflammatory cytokines and chemokines, initiating and coordinating the immune response in the CNS (DiSabato et al., 2016; Jain et al., 2020). This activation assists in recruiting peripheral immune cells, changing receptor expression, and promoting microglial movement toward areas of injury (DiSabato et al., 2016).

Astrocytes also have a crucial role in regulating neuroinflammation. After CNS injuries, they become reactive, influencing the secretion of extracellular matrix (ECM) molecules and assisting in the creation of a glial scar as a likely defensive mechanism to contain harm and restrict the infiltration of leukocytes (Ghorbani & Yong, 2021). Pro-inflammatory cytokines further encourage ECM production, reinforcing the development of the scar. Additionally, reactive astrocytes release saturated fatty acids that cause the death of oligodendrocytes, connecting disrupted lipid metabolism to neurotoxicity (Razo et al., 2024). The accumulation of lipid droplets in astrocytes can also activate microglia, further adjusting the inflammatory environment (Razo et al., 2024).

Various brain injuries like stroke, head trauma, and lesions from multiple sclerosis (MS) provoke an immediate neuroinflammatory reaction, often resulting in prolonged infiltration of leukocytes and persistent inflammation (Wilcoxon et al., 2002). The acute cytokine response (ACR), mostly regulated in the liver, produces cytokines, chemokines, and acute-phase proteins that prepare leukocytes for entering the CNS (Campbell et al., 2003). Extracellular vesicles (EVs) released by

astrocytes also contribute to this process, intensifying interleukin-1β (IL-1β)-mediated inflammation. The outcomes of neuroinflammation rely on its strength and duration. While a short-term, controlled response aids in tissue repair and immune protection, persistent or excessive activation can become pathological, leading to neurodegeneration (DiSabato et al., 2016). Prolonged T-cell interactions with CNS-resident cells, particularly microglia and astrocytes, are at the core of conditions like MS, where ongoing inflammation results in the demyelination of axons and gradual neurological deterioration (Rebelo et al., 2021; Podbielska et al., 2021).

2.1.3 Blood-brain barrier (BBB) in Neuroinflammation

The blood-brain barrier (BBB) is crucial for maintaining the balance of the central nervous system (CNS) by controlling the transfer of substances between the brain and the rest of the body (Hansen & Wang, 2023). It consists mainly of small blood vessel cells that create a specialised barrier. This selectivity is important for safeguarding the CNS, shielding it from harmful compounds, and managing the flow of ions, substances, and immune cells (Rebelo et al., 2021).

Basement membranes along the blood vessels in the brain support the BBB's integrity. These membranes are mainly made up of various proteins and molecules such as collagens, laminins, and heparan sulphate proteoglycans, which help uphold the structural strength and selective permeability of the BBB. In normal conditions, the BBB effectively regulates the passage of different substances to ensure the CNS functions properly and maintains its sensitive environment body (Hansen & Wang, 2023).

In conditions involving neuroinflammation, like stroke, multiple sclerosis (MS), or traumatic brain injury (TBI), the BBB may weaken (Hansen & Wang, 2023; Rebelo et al., 2021). This weakening allows white blood cells and unwanted molecules to enter the CNS, which contributes to ongoing nerve cell damage. In MS, the compromised BBB permits immune cells, such as T cells, B cells, and macrophages to access the CNS, escalating inflammation and causing further harm to nerve tissue and cells.. These processes are significant in driving the advancement of MS and the nerve cell degeneration seen in the disease (Hansen & Wang, 2023).

2.1.4 Neuroinflammation's role in MS pathology

Neuroinflammation is a central pathological process across various central nervous system (CNS) disorders, but its role in MS is particularly pronounced due to its contribution to both acute and chronic disease mechanisms (Razo et al., 2024; DiSabato et al., 2016). In MS, neuroinflammatory activity drives the destruction of myelin sheaths, which can lead to axonal injury or contribute to irreversible neurodegeneration. These mechanisms culminate in the formation of sclerotic plaques hardened lesions that represent the defining histopathological feature of the disease (Razo et al., 2024; DiSabato et al., 2016). The chronic presence of neuroinflammation is also implicated in the progression of other neurodegenerative conditions such as Alzheimer's disease (AD), where it leads to axonal fragmentation, cognitive decline, and motor impairments (DiSabato et al., 2016).

In MS, the immune system initiates a complex cascade of cellular events that result in inflammation and tissue destruction within the CNS. This response is driven by both innate and adaptive immune mechanisms, involving the activation and infiltration of T cells, B cells, and CNS-resident microglia (Razo et al., 2024). The pathological hallmark of MS, the demyelinated plaque, is characterised by focal loss of myelin and the presence of activated glial cells. These plaques are often bordered by areas of gliosis, where astrocytes become reactive and contribute to inflammation through the secretion of pro-inflammatory cytokines and chemokines (Belloli et al., 2018). The most affected regions include the optic nerves, spinal cord, brainstem, cerebellum, periventricular white matter, and corpus callosum, reflecting the widespread nature of MS pathology throughout the CNS white matter (Belloli et al., 2018).

Compromise of the blood-brain barrier (BBB) is another key feature of MS pathology. The integrity of cerebral vessel walls is frequently disrupted in chronic active lesions, where deposition of blood-derived proteins such as fibrinogen and fibronectin occurs on and around endothelial cells. This deposition is believed to facilitate the infiltration of peripheral immune cells into the CNS, further promoting inflammation and lesion formation. The accumulation of these proteins may also act as molecular signals that exacerbate microglial activation and neurotoxicity. (Ghorbani & Yong, 2021)

Once inside the CNS, immune cells contribute to oligodendrocyte apoptosis and axonal degeneration through a variety of cytotoxic pathways. Microglia and astrocytes play a central role in mediating this neuroinflammatory response. These glial cells release pro-inflammatory cytokines, reactive oxygen species (ROS), and other neurotoxic factors that perpetuate local tissue damage (Rebelo et al., 2021; Podbielska et al., 2021). The resulting inflammatory environment not only

accelerates demyelination but also impairs remyelination by inhibiting oligodendrocyte progenitor cell differentiation (Ghorbani & Yong, 2021). Sustained neuroinflammation and its downstream effects are strongly correlated with the progressive accumulation of neurological disability in MS patients (Podbielska et al., 2021).

2.1.5 Experimental Autoimmune Encephalomyelitis (EAE) model in MS research

The Experimental Autoimmune Encephalomyelitis (EAE) model is a widely used animal model to study MS preclinically. The model is both used to study immune research and for the development of anti-inflammatory treatments (Voskuhl & MacKenzie-Graham, 2022; Hasselmann et al., 2017). There are different versions of the EAE model, including monophasic, relapsing, and chronic forms. Chronic EAE mimics MS pathology broadly, indicated by white matter lesions in the spinal cord and grey matter atrophy, and is induced by myelin oligodendrocyte glycoprotein (MOG) peptide (Voskuhl & MacKenzie-Graham, 2022). This more conventional EAE model presents randomly distributed and multifocal lesions in the spinal cord, which may complicate analysis and cause unnecessary suffering within the rodents (Kalkowski et al., 2021).

Local Autoimmune Encephalomyelitis (LAE) is a newer MS model, which allows for precise lesion placement. The model involves immunizing the animal and inducing a demyelinating lesion through stereotactic injection of vascular endothelial growth factor (VEGF), which causes BBB leakage. (Kalkowski et al., 2021). This research has utilized a striatal LAE model, which has the advantage of generating large, consistent, and precise MS-like lesions.

2.1.6 Relevance of the striatum in MS

The striatum is a relevant region to study neuroinflammation in MS-like lesion models due to its involvement in various neurological disorders with neuroinflammatory components. Emerging evidence supports the presence of demyelination, neuroinflammation, and biochemical alterations within the striatum of both MS patients and animal models (Rebelo et al., 2021). In preclinical models of MS, particularly the experimental autoimmune encephalomyelitis (EAE) mouse model, the striatum has been shown to exhibit pronounced microglial activation, indicated by increased uptake of the ligand 18f-VC701 (Belloli et al., 2018). 18f-VC701 is a radioligand that binds to the

Translocator Protein (TSPO), which is upregulated in activated microglia. Its increased uptake reveals localised neuroinflammation (Belloli et al., 2018).

A different model using lipopolysaccharide (LPS) to induce neuroinflammation in the rat striatum has demonstrated significant changes in N-glycosylation, a post-translational modification of proteins (Rebelo et al., 2021). The striatum showed increased expression of inflammatory markers such as the TSPO, GFAP, and Iba1 upon LPS injection, indicating a localised neuroinflammatory reaction in the region (Rebelo et al., 2021). GFAP is an astrocyte marker, Iba1 marks microglia, and together with TSPO, these indicate increased expression signals of an active glial response (Rebelo et al., 2021).

The striatum was purposefully selected as the site of interest for inducing inflammatory brain injury in this study due to several methodological and biological considerations. Beyond its utility as a site for experimental induction of neuroinflammation, the striatum holds clinical significance due to its integral role in motor and cognitive function. The striatum is central to the basal ganglia circuitry, which controls movement and reward-based learning. Its dysfunction in MS may underlie symptoms like executive function and bradykinesia: loss of voluntary movement. (Ferreira et al., 2020).

The striatum is anatomically distant from the meninges, a connective tissue layer that covers the brain and spinal cord. Avoiding the meninges ensures that the inflammatory response studied originates from within the brain parenchyma and is not influenced by meningeal inflammation, which is common in some MS models (Voskuhl & MacKenzie-Graham, 2022). Moreover, the striatum's responses to pro-inflammatory agents such as cytokines and endotoxins have been extensively characterised, making it a reliable site for investigating inflammatory mechanisms Razo et al., 2024). Lastly, producing a precise lesion using the LAE has shown no clinical symptoms; a lack of overt signs greatly limits the suffering of the animals (Dickens et al., 2017). Thus, studying inflammatory responses and lesion development in the striatum not only provides insights into disease mechanisms but may also aid in understanding the functional consequences of deep grey matter involvement in MS (Voskuhl & MacKenzie-Graham, 2022).

2.2 Lipidomics for neuroinflammation

2.2.1 Role of lipids in the CNS

Neuroinflammation disrupts lipid homeostasis and metabolism, altering the lipid profile of the central nervous system (Ferreira et al., 2020; Yoon et al., 2022). In inflammatory demyelination, changes in myelin lipids impair sheath integrity and neural function (Podbielska et al., 2021). Oxidative stress induced by inflammation causes lipid peroxidation, compromising membrane stability (Ferreira et al., 2020).

Lipids account for about 50% of the brain's dry weight and are essential for structural and signalling roles in neuronal tissue (Trim et al., 2008). Lipidomic profiling provides insights into pathological processes in neurodegenerative and neuroinflammatory diseases such as multiple sclerosis (Fernández-Beltrán et al., 2021). Disruptions in lipid metabolism are associated with disease progression in CNS disorders (Trim et al., 2008). In MS, altered lipid metabolism is closely linked to inflammatory processes in the brain (Fernández-Beltrán et al., 2021). Mass spectrometry imaging (MSI) enables spatial mapping of lipid species within the CNS, allowing regional comparisons between lesions and unaffected tissue (Sjövall et al., 2004). Spatial lipidomics can reveal how specific lipid classes are modulated by inflammation and identify potential intervention targets (Podbielska et al., 2021).

MSI studies have shown that lipid distributions in the brain are regionally distinct and heterogeneous (Sjövall et al., 2004). Cholesterol and phosphatidylcholine exhibit complementary spatial patterns across brain structures (Sjövall et al., 2004). Sulfatides and phosphatidylinositol also display region-specific localisations that reflect underlying tissue biology (Sjövall et al., 2004). Principal component analysis (PCA) of MSI data highlights anatomical variation in lipid composition, with ion distributions strongly influenced by local tissue architecture (Sjövall et al., 2004).

2.2.2 Lipid alteration in neuroinflammation

Alterations in polyunsaturated fatty acids (PUFAs) has been shown to lead to changes in membrane composition, which influence signalling in neuroinflammation. These structural shifts affect the production of eicosanoids, lipid mediators made from fatty acids like arachidonic acid (AA), eicosapentaenoic acid (EPA), and docosahexaenoic acid (DHA). Eicosanoids shape inflammation

by either amplifying or dampening immune responses, depending on origin, with AA-derived mediators typically being pro-inflammatory and EPA/DHA-derived mediators acting anti-inflammatory. Lastly, acylcarnitines, a fatty acid involved in transportation into mitochondria, can accumulate during neuroinflammation. (Razo et al., 2024)

Phospholipids like phosphatidylethanolamine (PE) and N-acyl-phosphatidylethanolamine (NAPE) increase during inflammation and may contribute to immune modulation via bioactive signalling roles (Oliveira-Lima et al., 2019; Razo et al., 2024). Cholesterol, essential for synapses and myelin, becomes pathological when its transport or metabolism is altered, enhancing inflammatory pathways (Hansen & Wang, 2023).

2.2.3 Other Changes in the brain during inflammation

Neuroinflammation disrupts multiple lipid classes, each contributing differently to pathology. Phospholipids, key components of neuronal and glial membranes, undergo both structural and abundance changes. Species like phosphatidylethanolamine (PE) and N-acyl-phosphatidylethanolamine (NAPE) are elevated in inflamed regions, with NAPEs potentially exerting anti-inflammatory effects by acting as precursors to endocannabinoids (Oliveira-Lima et al., 2019; Razo et al., 2024).

Cholesterol, essential for myelin and synaptic stability, becomes pathological when uptake and signalling are dysregulated, which can amplify inflammatory cascades (Hansen & Wang, 2023). Mitochondrial lipid metabolism is also impaired. These changes further exacerbate oxidative damage and immune activation. Lipid droplets accumulate in astrocytes when fatty acid degradation is impaired. These droplets act not just as lipid reservoirs but as pro-inflammatory hubs that link metabolic dysfunction to degeneration (Mi et al., 2023).

Lipid signalling molecules are also centrally involved in modulating the neuroinflammatory milieu. Bioactive lipids such as prostaglandins, platelet-activating factor, and docosanoids, including neuroprotectin D1, are produced during inflammation and serve diverse roles. While some promote the initiation of the immune response, others facilitate its resolution and tissue repair. The balance between these opposing signals is crucial for the outcome of neuroinflammatory processes (Bazan, 2005).

2.2.4 Lipid dysregulation in neurodegenerative disorders

Lipid dysregulation is a prominent feature in several neurodegenerative diseases, including MS, Alzheimer's disease, and Parkinson's disease. These diseases are often associated with the accumulation of specific lipid species or disruptions in the balance of lipid metabolism, which contribute to neuronal damage and disease progression (Fernández-Beltrán et al., 2021). For example, a biomarker of Alzheimer's is a decrease of 40% phosphatidylethanolamine (PE) levels.

In MS patients, alterations in lipid composition can be detected in both plasma and cerebrospinal fluid (CSF), providing clues about the disease's progression and severity. Specific lipid imbalances in MS, such as those involving sphingolipids, glycerophospholipids, and cholesterol metabolites, have been linked to demyelination and neurodegeneration. Additionally, certain fatty acid species, like ω-3 polyunsaturated fatty acids (PUFAs), have been shown to exert protective effects against neurodegeneration by modulating inflammation and promoting cellular repair (Yoon et al., 2022). Ceramides play a role in sphingolipid metabolism and have been found to accumulate in MS lesions. These insights underscore the potential of targeting lipid metabolism as a therapeutic strategy for MS and other neurodegenerative conditions.

2.3 Lipidomics for MS diagnosis and therapy

2.3.1 Lipidomics and its role in Multiple Sclerosis

Lipidomics, which involves the comprehensive analysis of lipid species and distributions, offers a promising tool for the diagnosis and treatment of MS. Lipids may be relevant markers, potentially useful in predicting or monitoring the course of MS, particularly in progressive types of disease (Podbielska et al., 2021). Using techniques such as MSI, researchers can examine lipid alterations in specific brain regions, including focal lesions in MS, and compare these to the contralateral side, thereby allowing for a more detailed understanding of disease mechanisms (Yoon et al., 2022).

Lipidomic profiling has the potential to identify biomarkers for disease progression, enabling earlier diagnosis and more targeted interventions (Ferreira et al., 2020). Moreover, lipidomics can help uncover novel therapeutic targets (Del Boccio et al., 2011). While results from clinical trials remain mixed, lipidomic approaches could aid in tailoring personalised therapies based on specific lipid imbalances in MS patients. The integration of lipidomics with artificial intelligence and

interdisciplinary research could further refine treatment strategies for MS, providing a more nuanced understanding of lipid roles in the disease (Momchilova et al., 2022).

Lipidomic analysis helps researchers detect specific lipid changes in the body that are associated with MS, which may support earlier and more accurate diagnosis (Ferreira et al., 2020). In clinical settings, lipid profiling can also be used to monitor disease progression, predict relapses, and evaluate whether treatments are working (Yoon et al., 2022). These insights may contribute to personalised medicine, where treatment is tailored to a patient's biological profile

2.3.2 Lipid changes observed in MS

Research in both human patients and animal models has revealed significant changes in lipid composition during MS. In human studies, levels of PUFAs, such as linoleic acid (FA 18:2) and arachidonic acid (FA 20:4), were found to be reduced in MS patients. In contrast, there was a compensatory increase in saturated fatty acids with shorter carbon chains. These imbalances may affect membrane integrity and promote inflammation. (Ferreira et al., 2020)

Additionally, changes in sphingolipid metabolism have been observed, including lower levels of sphingomyelin and higher levels of ceramide and sphingosine, which are lipids involved in cell signalling and inflammation (Momchilova et al., 2022). In animal models of traumatic brain injury, used as a model for neurodegeneration, oxidised phospholipids and region-specific lipid changes have also been reported. For example, reduced levels of phosphatidylcholine (PC) and PE were found in the cortex and cerebellum, with increased levels in the hippocampus (Mallah et al., 2018).

In MS and other neuroinflammatory or lesion-associated conditions, a variety of lipid species are found to be altered, reflecting both disease activity and lesion type. This suggests an upregulation of sphingolipid biosynthesis during periods of active demyelination and inflammation. In the cerebrospinal fluid (CSF) of MS patients, ceramide species, including C16:0- and C24:0-ceramide, as well as C16:0-hexosylceramide, are notably elevated, further indicating systemic alterations in sphingolipid metabolism during disease progression. (Podbielska et al., 2021)

2.3.3 Challenges in lipid biomarker research

Despite promising findings, there are still significant challenges in identifying consistent and reliable lipid biomarkers for MS. Translating results from animal studies to human disease is complicated by differences in lipid metabolism and the complexity of MS pathology (Mallah et al., 2019). Furthermore, lipidomic data from different human sample types such as plasma, cerebrospinal fluid (CSF), red blood cells, and immune cells often yield inconsistent results (Ferreira et al., 2020). Even within the same sample type, results can vary due to differences in methodology and patient variability (Ferreira et al., 2020).

To address these issues, researchers recommend using both untargeted (broad) and targeted (specific) lipidomic techniques on the same sample type. This could improve reproducibility and allow for more meaningful comparisons across studies (Mallah et al., 2019).

2.3.4 Therapeutic targeting of lipid metabolism

Targeting lipid metabolism may offer new strategies to reduce inflammation and slow MS progression. One promising approach involves ceramide-1-phosphate (C1P), a signalling lipid known to promote inflammation. Reducing C1P levels may help decrease inflammatory responses in the central nervous system (Podbielska et al., 2021). Another experimental strategy involves blocking fatty acid oxidation, the process by which fats are broken down for energy. Inhibitors like Etomoxir are being tested to see if disrupting this metabolic pathway can reduce inflammation (Mi et al., 2023).

Another key pathway involves eicosanoids, which are inflammatory molecules made from arachidonic acid (AA), a type of PUFA. Enzymes called phospholipases, particularly phospholipase A2, release AA from cell membranes to begin the inflammatory cascade. Dysregulation of these enzymes and pathways has been observed in early stages of neurodegenerative diseases, such as amyotrophic lateral sclerosis (ALS), and may also be relevant in MS (Fernández-Beltrán et al., 2021; Oliveira-Lima et al., 2019). Further understanding of how these lipid pathways are regulated in the central nervous system could help identify early disease triggers and lead to new drug targets.

2.3.5 Lipid-targeted therapies in MS

Lipids are not only structural components of cellular membranes but also critical regulators of immune signalling, making lipids central to the pathogenesis of multiple sclerosis (MS). Growing evidence has demonstrated that targeting lipid metabolic pathways can modulate neuroinflammation and thus offer promising pharmacological strategies for MS treatment (Podbielska et al., 2021; Mi et al., 2023).

The best-established examples are the use of sphingosine-1-phosphate receptor (S1PR) modulators. Fingolimod, the first drug approved in this class, reduces inflammation by preventing lymphocyte migration into the central nervous system (CNS) and promoting immune cell apoptosis (Podbielska et al., 2021). More recent S1PR modulators, such as ozanimod and ponesimod, selectively target S1PR1 and S1PR5, thereby reducing immune activity while also supporting potential mechanisms of myelin repair. Siponimod, another S1PR-targeting agent, has shown specific efficacy in secondary progressive MS (SPMS), where it exerts both anti-inflammatory and neuroprotective effects (Podbielska et al., 2021).

Other lipid-modulating therapies include dimethyl fumarate (DMF), widely used for relapsing-remitting MS (RRMS). DMF works by activating antioxidant pathways, thereby reducing oxidative stress and modulating immune responses within the CNS. Targeting lipid metabolism offers several potential strategies to reduce inflammation in MS. One approach involves Cer 1-phosphate (C1P), which mediates pro-inflammatory activities; reducing C1P levels may diminish inflammation (Podbielska et al., 2021). Inhibiting fatty acid oxidation with drugs like Etomoxir is another strategy being tested experimentally to disrupt lipid metabolism (Mi et al., 2023).

Insights from related neurological disorders support this therapeutic direction. For instance, in ALS, eicosanoid signalling, particularly involving arachidonic acid (AA), has been found dysregulated early in disease progression (Fernández-Beltrán et al., 2021; Oliveira-Lima et al., 2019). These inflammatory lipids are generated by phospholipase A2, enzymes that are also elevated in the CNS of ALS patients and animal models, pointing to shared lipid-mediated inflammatory pathways in neurodegeneration (Fernández-Beltrán et al., 2021).

The use of advanced imaging methods, such as mass spectrometry imaging (MSI), has enabled researchers to track lipid alterations in situ. In LPS-induced models of neuroinflammation, MSI revealed specific lipid species accumulating in inflamed brain regions (Razo et al., 2024). Among lipids, N-acyl-phosphatidyl-ethanolamines (NAPEs) co-localise with activated microglia and may

engage in endocannabinoid signalling pathways, potentially mediating neuroprotection. Other lipid species, such as polyunsaturated fatty acids (PUFAs) and acylcarnitines, have also been implicated (Razo et al., 2024). While PUFAs are thought to give rise to specialised pro-resolving mediators that help resolve inflammation, acylcarnitines are markers of impaired mitochondrial β-oxidation and may drive sustained immune activation (Razo et al., 2024).

Elevated levels of acylcarnitines in proximity to injury sites indicate disruptions in carnitine transport and the mitochondrial β-oxidation pathway. These lipid species may also participate in initiating or sustaining a pro-inflammatory response under neuroinflammatory conditions (Razo et al., 2024). Together, these findings reinforce the potential of lipid metabolism as both a window into disease mechanisms and a target for therapeutic intervention in MS (Razo et al., 2024).

2.4 Imaging techniques

2.4.1 MSI imaging or spatial lipidomics

This thesis focuses on lipidomics, the study of lipids, using Matrix-Assisted Laser Desorption/Ionization - mass spectrometry imaging (MALDI-MSI). Lipidomics is instrumental in understanding how different lipids contribute to neurodegenerative diseases like multiple sclerosis (MS) (Rebelo et al., 2021). Lipids are key regulators in neuroinflammation through roles in maintaining cell membrane integrity, signalling pathways, and energy storage. When lipid regulation is disrupted, it can contribute to inflammation, immune cell activation, and neuronal damage (Mallah et al., 2019).

MALDI-MSI is a powerful imaging technique that enables researchers, among other things, to map lipid distributions across different brain regions with high spatial resolution. Unlike other biochemical methods that analyse lipids in bulk tissue samples, MALDI-MSI enables the visualization of lipid changes at specific anatomical locations. (Rebelo et al., 2021; Trim et al., 2008). This is particularly valuable for studying neuroinflammation, where localized lipid alterations may indicate disease progression, immune cell infiltration, or tissue damage (Mallah et al., 2019; Podbielska et al., 2021). By identifying lipid markers associated with inflammation, this technique provides insights into the molecular mechanisms underlying neuroinflammation (Rebelo et al., 2021).

A major strength of MALDI-MSI is its ability to detect a broad range of biomolecules in an untargeted, label-free manner, capturing mass spectra at each pixel and enabling spatially resolved MSI-level lipidomics. This approach reveals lipid heterogeneity across tissues and cell types, reflecting diverse roles in membrane biology, signalling, and pathology. Lipids are particularly suited to MSI due to high abundance, efficient ionization, and straightforward sample preparation, which enhances reproducibility. Compared to proteins or metabolites, lipid MSI offers robust spatial lipid profiling, making it a powerful tool for diagnosing or characterizing disease-linked alterations in tissue lipid composition (Bowman et al., 2019).

2.4.2 Principal Component Analysis in MSI

PCA is a widely used multivariate statistical technique for analysing complex lipidomics datasets, particularly in lesion studies using Mass Spectrometry Imaging (MSI) (Mallah et al., 2019). PCA helps visualize lipidomic profile differences between experimental groups (Mi et al., 2023). It reduces data dimensionality and identifies variance sources (Mi et al., 2023). In TBI studies, PCA distinguishes injured from uninjured tissue, though not always between different injury time points (Mallah et al., 2019). PCA models spectral profile differences in injured brain regions, aiding cluster separation based on lipid profiles (Mallah et al., 2019).

Two key graphical outputs of PCA are the score and loading plots (Mallah et al., 2019. This visualization enables the identification of clustering patterns, trends, and separation between experimental groups, revealing underlying biological variability (Trim et al., 2008). In the context of lipidomics MSI, the score plot is particularly useful for assessing whether lesion areas exhibit distinct lipid profiles compared to healthy regions. If well-separated clusters are observed, this indicates systematic lipidomic differences driven by the lesion pathology (Trim et al., 2008).

In contrast, the loading plot shows which specific lipids contribute most to these differences, acting as potential biomarkers (Mallah et al., 2019). The loading plot helps identify which lipids drive overall variance but does not directly indicate group differences. Instead, separation between lesion and non-lesion regions is seen in the score plot, where sample clustering reflects group differences (Mallah et al., 2019). If the lesion and healthy samples form separate clusters, it means the lipid profiles are different. When used together, these plots help link specific lipids to observed differences, making the loading plot valuable for biomarker discovery, especially in studying

inflammation. Ideally, both should be shown: the score plot displays sample grouping, while the loading plot explains the molecular basis of these differences (Trim et al., 2008).

Confidence ellipses visualize data spread, indicating data reliability and group separation (Mallah et al., 2019). To visualize data spread, 95% confidence ellipses can be included. In the loading plot, these ellipses highlight which lipids contribute most to variance. Within the scoring plot, the distinctness of ellipses reflects group separation; the more distinct and non-overlapping the ellipses are, the greater the differences or variability between groups (Mallah et al., 2019). The size of each ellipse indicates within-group variability: larger ellipses mean more variation, while smaller ones suggest more uniformity within a group.

2.4.3 PET imaging

PET imaging is a non-invasive method for assessing metabolic activity in living tissues, making it useful for monitoring inflammatory processes in vivo (Podbielska et al., 2021). Brain tissue slides for MALDI-MSI were collected from an experiment integrating Positron Emission Tomography (PET) and autoradiography.

In this experiment, mice received MS-like lesions and had 18F-NFL, a neurofilament light chain (NFL) tracer, injected directly at the lesion site to assess neuroinflammatory damage. NFL is a structural protein found in neurons, and elevated levels serve as a biomarker for neuronal damage and axonal degeneration both in the CNS and the rest of the body (Podbielska et al., 2021). Injecting the tracer at the lesion or sham-lesion site enabled the detection of areas with increased NFL in the body, offering insights into brain-periphery communication and inflammatory progression (Jain et al., 2020).

Although the results of PET imaging and autoradiography are not detailed in this thesis, there might be an impact on the results of MALDI-MSI data that must be acknowledged.

2.4.4 Study of neuroinflammation integrating both imaging approaches

Lipidomic analysis is valuable for understanding neuroinflammation in multiple sclerosis (MS) as alterations in lipid metabolism and individual lipid molecular species play significant roles in MS pathogenesis and disease severity (Ferreira et al, 2020). Changes in the lipid profile are a hallmark

of MS, contributing to dysregulation of lipid homeostasis and metabolism (Ferreira et al, 2020). Specifically, lipidomic studies have demonstrated the role of lipids in inflammatory processes, immunity, and the onset and development of MS (Ferreira et al, 2020). Lipidomics allows for the evaluation of lipid variations at a molecular level, serving as important biomarkers for the disease (Ferreira et al, 2020).

To strengthen the understanding of these pathological mechanisms, lipidomic profiling can be combined with advanced neuroimaging modalities such as Positron Emission Tomography (PET) (Belloli et al., 2018). PET imaging provides longitudinal visualization and the tracking of inflammatory markers in living subjects (Jain et al., 2020). For example, previous work using PET with translocator protein (TSPO) ligands, such as 18F-VC701, has demonstrated the utility of PET in detecting microglial activation and neuroinflammation in MS models. The increased uptake of the TSPO ligand 18F-VC701 in a mouse model of MS was strongly associated with microglial activation, a key component of neuroinflammation (Belloli et al., 2018). Lipidomic ex vivo analysis integrated with in vivo PET analysis could significantly enhance the understanding of lipid dynamics during neuroinflammation (Belloli et al., 2018).

2.4.5 Hypotheses

This thesis investigates the lipidomic alterations associated with experimental demyelinating lesions in the striatum, modelled to reflect aspects of multiple sclerosis (MS) pathology. The overarching hypothesis is that striatal lesions induce both localised and systemic changes in lipid expression, which can be detected and characterised using mass spectrometry imaging (MSI). These lipidomic shifts are expected to reflect disruptions in membrane composition, signalling pathways, and contribute to neuroinflammatory processes.

Given the known roles of phosphatidylcholines (PC), phosphatidylethanolamines (PE), diacylglycerols (DG), and ceramides in neuroinflammation, demyelination, and membrane remodelling, it is hypothesized that these lipid classes will show altered abundance in lesioned tissue relative to controls. Although the analysis was limited to a targeted panel of 70 lipids, it is expected that key representatives from these classes will demonstrate either localised enrichment or depletion corresponding to lesion-induced pathology.

The specific aims of this study are as follows:

- To identify localised lipidomic changes associated with striatal lesions, by comparing lipid abundance in the lesioned left striatum to the anatomically corresponding region in sham-operated animals.
- To assess systemic or hemispheric alterations in lipid expression by comparing lipid profiles from both hemispheres of lesioned animals to those of sham controls.
- To evaluate intra-subject lipid distribution by comparing the lesioned and contralateral striata within the same animals, thereby controlling for local versus brain-wide neuroinflammation.
- To apply multivariate analysis (PCA) to explore trends and lipid contributions beyond univariate significance, to identify lipid species that, while not individually significant in hypothesis testing, contribute strongly to group separation and may reflect coordinated biochemical responses to lesioning.

Collectively, these analyses aim to provide a spatially resolved understanding of lipid dysregulation in a striatal lesion model, offering insights into the molecular underpinnings of demyelination and potential targets for further investigation in neurodegenerative disease contexts.

3 Methodology

3.1 Experiment

3.1.1 Animals

This experiment involved 19 C57BL/6 mice, with an average age of three months. C57BL/6 mice were selected due to the well-characterised neuroinflammatory responses and genetic consistency (Belloli et al., 2018). Most subjects were male (n=18). The mice were divided into two experimental groups: lesion (n = 19, excluding deceased) and sham (n = 6). The mice were kept in the laboratory housing facilities under controlled conditions, with a temperature of approximately 21 °C, humidity of 45-60 %, and a 12-hour light/dark cycle. The mice were weighed before PET imaging and had an average weight of 295 g (±4.1 g). Food and water were provided ad libitum to ensure proper nutrition. The housing conditions followed in this study adhere to guidelines provided in the Laboratory Animal Welfare Course by the Turku Center for Disease Modeling (TCDM) (2024). TCDM holds all necessary licenses for studies in experimental animals approved by the Finnish Animal Ethics Committee, and the institutional policies on animal experimentation fully meet the requirements as defined in the NIH Guide on animal experimentation (Turku Center for Disease Modeling, 2024).

Table 1: List of mice involved in PET imaging, a selection of animals was later used for MSI imaging.

Date	Animal	Group	Sex	Date of birth	Weight
08/12/2023	OXF1	Lesion	M	28/09/2023	0.027
08/12/2023	OXF2	SHAM	M	15/09/2023	0.026
08/12/2023	OXF3	Lesion	M	28/09/2023	0.028
08/12/2023	OXF4	SHAM	F	15/09/2023	0.020
13/12/2023	OXF5	Lesion	M	28/09/2023	0.032
13/12/2023	OXF6	SHAM	M	28/09/2023	0.022
13/12/2023	OXF7	Lesion	M	06/06/2023	0.036
13/12/2023	OXF8	SHAM	M	28/09/2023	0.029
14/12/2023	OXF9	Lesion	M	06/06/2023	0.033
14/12/2023	OXF10	SHAM	M	28/09/2023	0.029
14/12/2023	OXF11	Lesion	M	28/09/2023	0.028
14/12/2023	OXF12	SHAM	M	28/09/2023	0.028
30/01/2024	OXF31	Deceased	M	02/11/2023	0.029
30/01/2024	OXF32	Lesion	M	02/11/2023	0.031
30/01/2024	OXF33	Lesion	M	02/11/2023	0.028
30/01/2024	OXF34	Lesion	M	02/11/2023	0.038
31/01/2024	OXF35	Lesion	M	02/11/2023	0.031
31/01/2024	OXF36	Lesion	M	02/11/2023	0.031
31/01/2024	OXF37	Lesion	M	02/11/2023	0.031

3.1.2 Immune Priming

The animals are first immunised using an intradermal injection in the leg (25 uL) with an emulsion of myelin oligodendrocyte glycoprotein (MOG) 35-55 peptide (0.5 mg/mL in saline; Innovagen, Sweden). This occurs approximately 26 days before imaging and sample acquisition. This combination disables the immune system, which leads to priming the brain for lesion formation. The sham control group received a sterile saline injection instead to control for any effects from the injection procedure itself.

3.1.3 Lesion Induction

Twelve days before sample collection, stereotactic surgery was performed on mice in the lesion group to create targeted lesions in the left striatum. All surgical procedures were completed while animals were under isoflurane gas (1.5% in 100% O2). Animals were checked to be properly anaesthetized by pinching the leg. The striatum was chosen due to its role in neuroinflammation and its dense dopaminergic and glutamatergic innervation, which are critical for motor and cognitive functions frequently affected in MS patients (Rebelo et al., 2021). Additionally, the induced inflammation does not cause overt behavioural changes that could impair the animal's ability to access food or water, nor does it lead to heightened pain sensitivity, which can occur when the lesion-inducing substance is injected more caudally (Dickens et al., 2017)

The head of the animal was shaved and sterilised, and the animal was placed in a stereotaxic frame (Stoelting Co.). A small (2mm) midline incision was then made in the scalp, and a burr hole was drilled 0.7 mm anterior and 2.7 mm lateral to the bregma using a dental drill (Fine Science Tools). With the use of a finely drawn glass microcapillary (< 50μm), 1 μL of heat-killed Tuberculosis (8.8 mg/mL in saline) is injected into the left striatum. The coordinates of the lesions were as follows: bregma +1.5 mm (anterior), lateral 1.0 mm, depth 2.5 mm (Wilcockson et al., 2002). After surgery, the wound was sutured, and the animals were allowed to recover in a thermostatically controlled chamber. Sham-control mice underwent an identical surgical procedure but received an injection of sterile saline instead of the lesion-inducing substance.

Lesion success was confirmed postmortem using autoradiography and MSI-based lipid imaging. In the autoradiography imaging, the concentration of the radiotracer NFL binding was visualized, overall showing strong binding in the left hemisphere, and less bright, indicating little NFL tracer

binding in the right hemisphere in lesioned animals. The MALDI-MSI ion images of lesioned animals revealed several ions with statistically significant differences in the left versus right striata. By looking at several of these distinct molecular differences, the exact locations of the lesions are beautifully visualized as seen in Image 1.

3.1.4 PET-CT Imaging and NFL Tracer Injection

On the day of sample collection, whole-body PET-CT imaging was conducted to track neuroinflammation and lesion progression. Mice were anesthetized using breathable isoflurane to ensure immobility throughout the procedure. The NFL tracer, a radiolabelled compound that binds to neurofilament light chain (NFL) proteins, was injected directly at the lesion site. NFL proteins are released during axonal damage, making NFL a useful biomarker for neuronal injury. By binding to these proteins, the tracer enables real-time visualization of affected brain regions in the PET scan. Each day, four mice underwent imaging and euthanasia, with two mice put in the PET scan simultaneously. During the procedure, one male mouse from the lesion group died, likely due to overheating while under anaesthesia. The PET-CT scan lasted for 120 minutes, during which the tracer's distribution in the brain and other body tissues was monitored. This helped to confirm lesion-specific uptake of the tracer while identifying any off-target binding.

3.2 MSI for spatial lipidomics

3.2.1 Sample acquisition

Immediately following the PET-CT scan, mice were euthanized through cardiac blood loss while still under anaesthesia. This ensured a humane and painless procedure and ensured tissue integrity for further analysis. Autopsies were performed behind lead shields, and collected brains were flash frozen using Isopentane on dry ice. Coronal brain slices of 10 µm thickness were created using cryo-sectioning under cold conditions (−20 °C). Brain tissues were placed on respective slides for autoradiography and MSI imaging by supervisors. Tissue for MSI was created using Super Frost™ Plus Adhesion charged slides, each containing approximately 5 brain slices with a thickness of 10µm, as seen in image x. MSI slides were transported to a (−20 °C) freezer until the imaging stage.

3.2.2 Tissue retrieval for MSI

The following steps are modified based on the standard operating procedure for MS analysis using Scilslab. Samples were stored at temperatures below -18°C in freezers without the NOFROST feature to prevent dehydration and minimize the risk of thawing. Proper sample handling was ensured by avoiding exposure to ambient conditions, which could introduce condensation or unintentional thawing.
To maintain sample integrity, a desiccator was used to transport the tissue slices to the laboratory. Samples were placed inside the desiccator so that minimal exposure to the external environment is ensured. The vacuum pump was attached and activated for a minimum of 30 minutes, allowing the samples to reach room temperature gradually while preventing condensation. Afterward, the vacuum was released slowly, and the samples were inspected for any signs of moisture.
Before the matrix application, optical images of the samples were obtained using a printer. Camera settings were adjusted to optimize brightness and contrast, and images were scanned and labelled according to sample number and date for tracking and reference, as seen in image 1.

Image 1: FlexImaging slide for MSI containing coronal brain tissue.

3.2.3 Matrix Application

For MALDI MSI, a thin, even layer of matrix is applied onto the brain tissue slides for lipid imaging, which facilitates analyte ionization efficiency (Fernández et al., 2018). The matrix solution used for this experiment is 2,5-Dihydroxybenzoic Acid (DHB) and was deposited onto the tissues using a sublimation apparatus. A sublimation apparatus produces uniform matrix crystals and ensures reproducibility and quality of ion images in MALDI-MSI experiments (Fernández et al., 2018).
The sublimation apparatus (Image 2) was prepared by assembling the inner and outer components and setting the initial temperature to 300 °C before reducing it to 200 °; once it had reached 140 °C. While the sublimater reached temperature, 750 µl DHB was pipetted into the inner chamber of the sublimater and evenly distributed using a nitrogen air blower. Samples were placed face down in the designated holder and

secured with adhesive foil. Ice was added to the sublimation chamber to maintain stability. Vacuum control was initiated gradually to reach an appropriate pressure. The system was allowed to stabilize for 15-20 minutes, until all matrix solution had cleared from the bottom and crystallized onto the tissue slide. Once ready, the vacuum was released, the machine turned off, and the slide recovered. Onto a tissue-free part of the matrix, ½ µl of red phosphor-acetone solution was applied as a calibration point. The slides were once more blasted with nitrogen to ensure there is no excess matrix before being placed into the sample carrier.

Image 2: Sublimiter to apply DHB matrix onto brain tissue slices.

3.2.4 MALDI imaging acquisition

Released ions were detected using a MALDI TimsTOF fleX trapped ion mobility separated QTOF mass spectrometer as seen in Image 3 (Bruker Daltonics, Germany). The sample carrier is carefully placed into the MSI machine. The imaging parameters were configured using the lipid profiling method (MALDI-1 TIMS-off positive 20µm) with a spatial resolution of 20µm for the optimal tissue slice, 50µm for the other acceptable-looking tissues. The sample carrier was generated, and height adjustments were performed automatically. Before data acquisition, laser settings were calibrated. The laser beam offset was adjusted automatically, and the focal point was aligned with the tissue matrix. The laser height was verified within a ±15 µm range to ensure optimal ionization conditions.

Calibration was performed using red phosphorus as a reference standard. The instrument's mass accuracy was confirmed with a calibration score of $\geq$ 98% and an intensity threshold above 2000 counts. For mobility calibration, an Agilent mix (a sodium formate cluster solution) was infused at a rate of 3 µL/min.

Voltage adjustments were made to achieve proper alignment at 164V. The laser energy was initially set at a low level and gradually increased until sufficient ionization was observed. For 20 µm resolution, a laser power of approximately 30% was optimal, whereas for 50 µm resolution, 15% was used. Signal peaks were monitored within the 500-5000 m/z range, with cholesterol detection at 369 m/z serving as a key validation marker.

Measurement regions were selected in FlexImaging software, with distinct outlines for 50 µm and 20 µm regions. Once all parameters were confirmed, the imaging run was initiated. A single imaging run takes approximately 14 hours per set of slides and was left to run overnight.

Image 3: Mass Spectrometer apparatus, figure adapted from The Hong Kong Polytechnic University (2025).

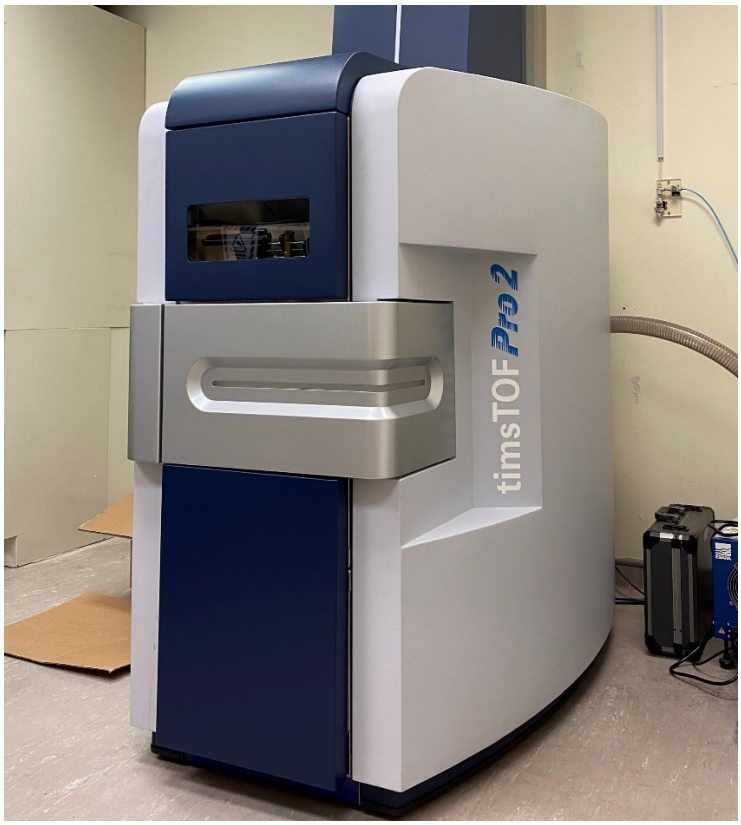

3.2.5 Preprocessing MSI data

Following data acquisition, raw imaging data were transferred from the instrument computer to the analysis workstation. The .mis files were imported into SCiLS Lab, ensuring all relevant datasets were included (SCiLS™ Lab, Bremen, Germany). Feature extraction and segmentation were performed, balancing spatial smoothing and processing time. Identified features were further analysed to generate ion images and segmentation maps. Examples of ion images are seen in images 1-3. For lipid identification, some were compared against reference lipid databases, enabling molecular annotation, whilst others were identified in SCiLS software, with the molecular weight calculated.

3.2.6 MALDI-MSI analysis

To maximize and visualize the variability of the data, PCA can be used. PCA can be seen as an automated extraction of the underlying trends within a dataset (Bruker Daltonics, Germany). PCA was performed between the left and right striata of the lesioned brain tissues and between the left striata of the lesioned versus sham control brains for both the 20µm and the 50µm pixel imaged slides using the SCiLS Lab Version 2025a Pro software. The settings were as follows: All MSI data were normalised to the total ion count (TIC), no denoising, Peak Area as interval processing mode, Root Mean Square for normalization, up to 5 components, scaling per Pareto, and the Mean Spectrum Mode. Pareto scaling uses the square root of the standard deviation to ensure lower abundance ions are not masked during PCA (Trim et al., 2008). All settings are per the laboratory's standard instruction manual / valued PhD student Ilia.

3.2.7 Hypothesis Testing

To evaluate lipidomic differences in the MSI study of lesioned brains, statistical comparisons were conducted both within subjects (left vs. right hemisphere) and between experimental groups (lesioned vs. sham animals). These analyses aimed to identify localized and systemic changes in lipid expression associated with striatal lesions. Before conducting group comparisons, it was assessed whether the lipid intensity data followed a normal distribution using the Anderson-Darling test, with statistical significance set at $p < 0.05$. The test yielded a p-value of 0.227, indicating that the assumption of normality could not be confidently upheld. Based on this result, non-parametric, rank-based statistical methods for hypothesis testing were chosen. Due to the non-normal distribution of the data, the Kruskal-Wallis test was employed to detect significant differences in lipid abundance across experimental conditions. The following comparisons were performed:

- Lesioned left striatum vs. sham striata: Lipid levels in the lesioned left striatum were compared to those in the left striatum of sham-operated animals to evaluate localized lesion effects.
- Both hemispheres of lesioned Brains vs. sham striata: Lipid levels from both the lesioned and contralateral striata were compared to those from sham subjects to assess broader hemispheric alterations.
- Lesioned vs. contralateral striatum (within lesioned animals): The lesioned left striatum was compared to the contralateral (right) striatum within the same subjects to determine whether lipid changes were confined to the lesion site or brain-wide.

3.2.8 Confirmation of Lipid Identity and Adduct Exclusion

To verify that statistically significant lipid features did not represent different adducts of the same molecular species, m/z values were examined for characteristic adduct mass differences (e.g., 22.989 Da for Na^+, 38.963 Da for K^+). No consistent adduct-related mass shifts were observed among significant features, confirming that the detected lipids represented distinct molecular entities rather than ionization artifacts or adduct variants.

Determining the exact molecule from an m/z value in lipidomics, especially for MS-like lesions, involves several steps. First, the accurate mass measurement is compared against lipid databases such as LIPID MAPS using a narrow mass tolerance (e.g., ±4 ppm) to generate a list of potential candidates (Mallah et al., 2019) (Lipid Metabolites and Pathways Strategy). Next, tandem mass spectrometry (MS/MS) is employed to fragment the molecule and generate a unique fragmentation pattern (Mallah et al., 2019). This fragmentation pattern is then matched against spectral libraries or predicted based on the known structure of candidate lipids (Mallah et al., 2019).

Spatial distribution in the sample aligned with known MS-like lesion locations, coupled with co-localization analysis, further strengthens lipid identification (Mallah et al., 2019). Additionally, preliminary assignments are confirmed through MS analysis on lipid extracts, comparing fragmentation patterns of the lipid against those of a standard (Mallah et al., 2019).

It is possible to identify lipids using accurate mass measurements and targeted lists, analysing MALDI MSI data without tandem MS, but with caveats. This study used a targeted list of lipids with formulas, so to confirm the first step is to calculate the exact mass of each lipid using its formula and compare these calculated masses to the experimental m/z values, again using a narrow tolerance. Assessment of the likelihood of each match based on known lipid distributions in brain tissue and MS-like lesions from published literature, and consider factors like ionization efficiency and matrix effects that might favour certain lipids (Mallah et al., 2019). The Consensus AI, a search engine one can use to discover published literature that answers a specific question, has been used to find papers supporting the research findings of this thesis.

4 Results

4.1 Rationale for sample exclusion

The following MALDI-MSI images show the spatial distribution of lipid species in a representative tissue slice from a lesioned or sham-control mouse. Image 4 shows a successfully processed lesioned mouse (slice 45), with clear elevated ion intensity marked with yellow, focused on the striatum of the left hemisphere corresponding to the MS-like lesion site. In Image 5, a sham-control mouse is displayed; the same lipid shows a symmetric distribution, consistent with the absence of pathology. Images 6 and 7 show examples of excluded brains, tissues 73 and 69, respectively. The tissue sections of 73 got warped during cryo-sectioning, whereas 69 exhibited abnormal ion distribution patterns and shape, inconsistent with biological expectations. These and other exclusions will ensure robust and meaningful MSI results. The inclusions and exclusions are detailed in Table 2.

Image 4: MALDI-MSI ion image of a mouse with MS-like lesion in the left hemisphere, brain slice number 45.

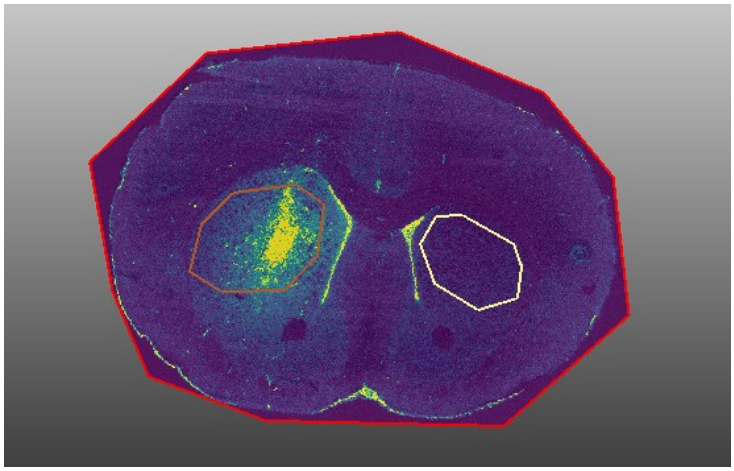

Image 5: MALDI-MSI ion image of a sham-control mouse, brain slice number 72.

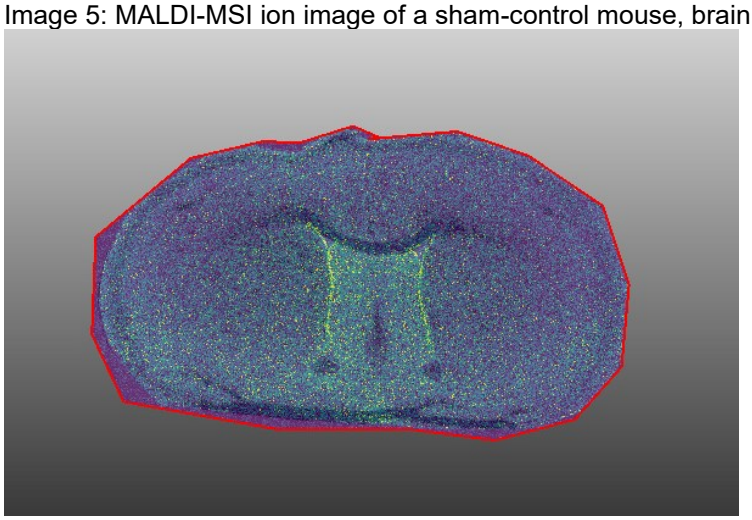

Image 6: MALDI-MSI ion image of lesioned mouse 73, tissue damage during cryostat slicing.

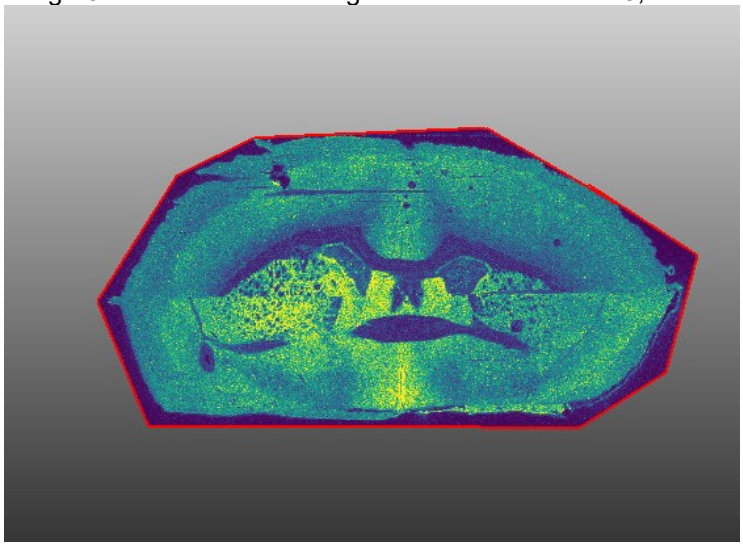

Image 7: Ion distribution at m/z 796.58 in lesioned animals, highlighting left striata; tissue slices from animal 69 display anomalous signal in pink.

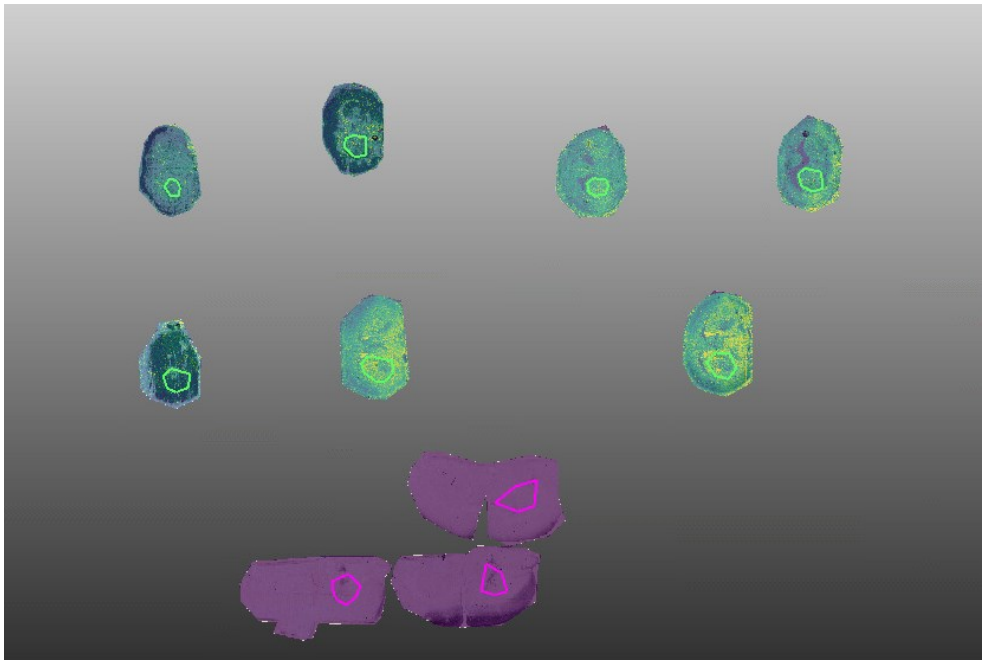

Table 2: Overview of Included and Excluded Samples for MALDI MSI Analysis.

Group	Sample Numbers	Excluded Samples	Reason for Exclusion
Lesioned mice	40, 44, 45, 48, 49, 50	46, 69	46: Faulty tissue slicing 69: Abnormal MSI data
Sham control mice	66, 67, 72	68, 73	68: Faulty tissue slicing 73: Poor MSI data quality

4.2 Averaged mass spectra comparison between groups

To assess and illustrate global ion distribution patterns between groups, averaged mass spectra images were generated for the striatal regions across different groups prior to multivariate analysis. These spectra provide an overview of molecular composition and can help interpret PCA results. Within non-lesioned animals, the averaged spectra from the left and right striata (peach and yellow traces, respectively) were nearly identical (Image 8), with overlapping ion profiles across the entire m/z range. This symmetry indicates no significant lateralized differences in baseline lipid composition, supporting the assumption of molecular uniformity of a specific brain region, like the striatum, under baseline, non-pathological conditions. Spectra overlays within the lesioned animals are compared to isolate lesion-specific effects. Within the lesioned animals, there is a clear contrast when comparing the spectra of ion intensities, it becomes clear that there are hemispheric differences between the lesioned left striata (yellow) and the contralateral right striata (green). Peaks corresponding to m/z 768.59 and 758.57 show lateralized changes in signal intensity within the lesion animals. These shifts indicate lesion-induced local alteration in feature abundance and composition, reflecting local changes due to the induced MS-like lesion.

Image 8: Averaged mass spectra of left (peach) and right (yellow) striata in non-lesioned animals.

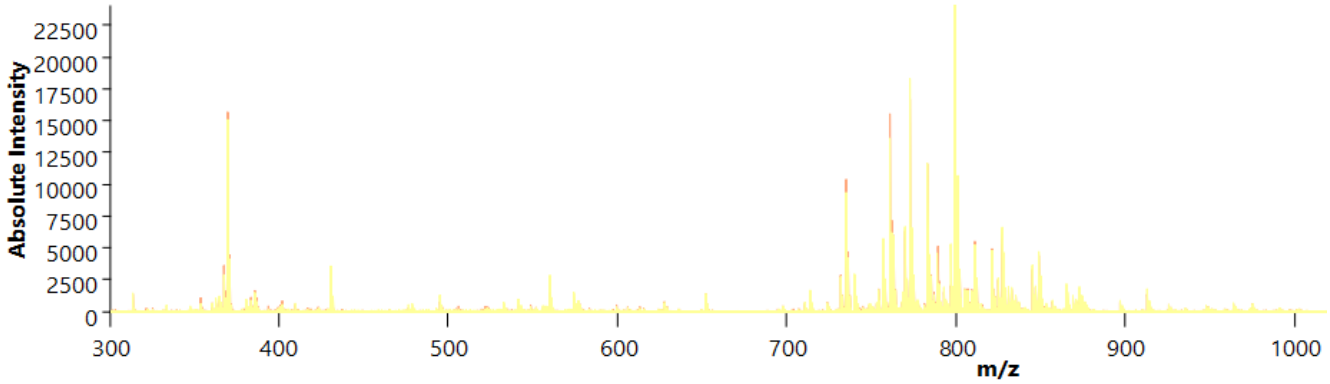

Image 9: Averaged mass spectra of lesioned striata (yellow) and contralateral striata (green).

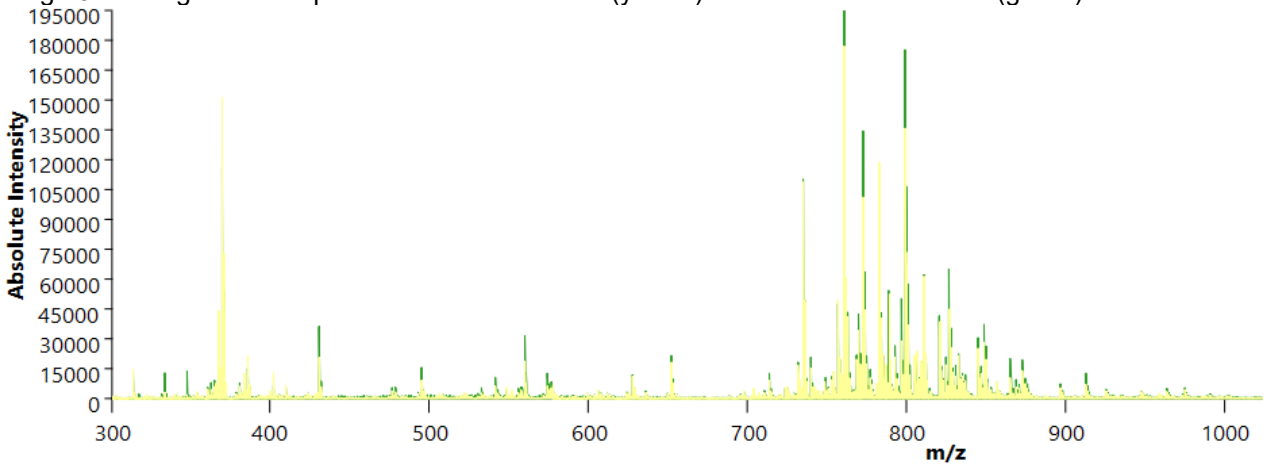

When comparing averaged spectra between the lesioned striata (yellow) and all sham striata (purple) in images 10 and 11, spectral divergence between the experimental groups can be observed. Several more ion intensity peaks appeared elevated or depleted in the lesioned regions compared to control tissues; ions around m/z 774, 806, 796, and 746 differed substantially in intensity. These lipids are later identified and confirmed to have statistically different abundance between groups. Overall, the divergence suggests lesion-induced alterations in lipid abundance due to the MS-like lesions.

Image 10 & 11: Averaged Mass Spectra of Left Lesioned Striata (yellow), and Sham Striata (purple)

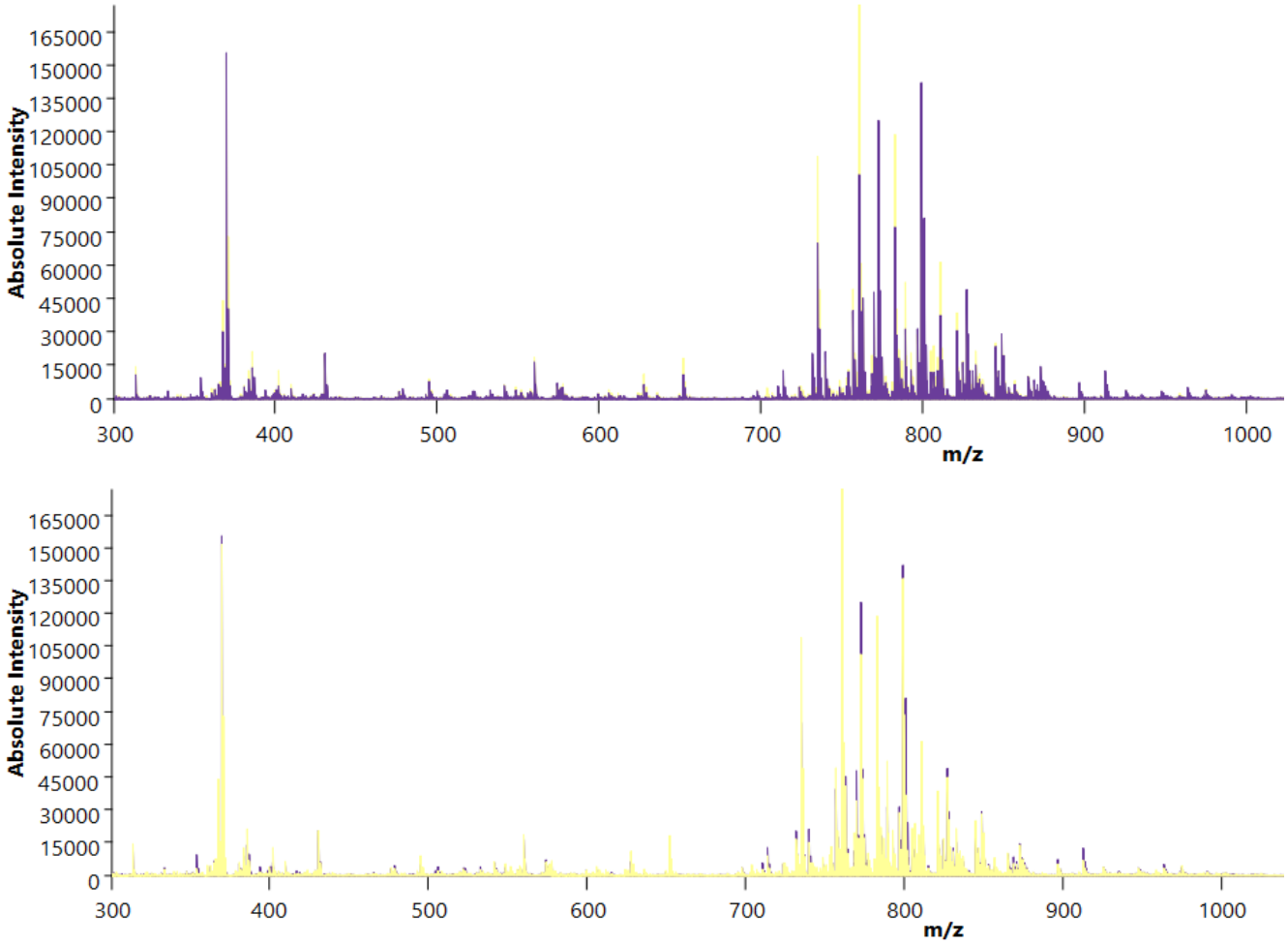

4.3 Scoring plots PCA

Images 12 and 13 depict the scoring plots of the MSI data. To recap, scoring plots visualize separation between experimental groups, revealing trends. Well-separated clusters indicated by more distinct confidence ellipses show systemic lipidomic differences driven by lesion pathology. Image 12 shows the PCA results within the lesioned animals, blue marks the left lesioned striata, and red marks the contralateral striata of the lesioned mice. Image 13 shows the PCA results between the control striata in yellow versus the lesioned striata in blue (with a purple confidence ellipse). The lesioned striata show more variability than the control striata, marked by the larger confidence ellipse. By comparing both scoring plots, it is clear that Image 12 shows less distinct confidence ellipses than Image 13, indicating more variability between the experimental groups than within the lesioned animals.

Image 12: PCA Scoring plot within lesioned brains, left vs right striata 50 µm.

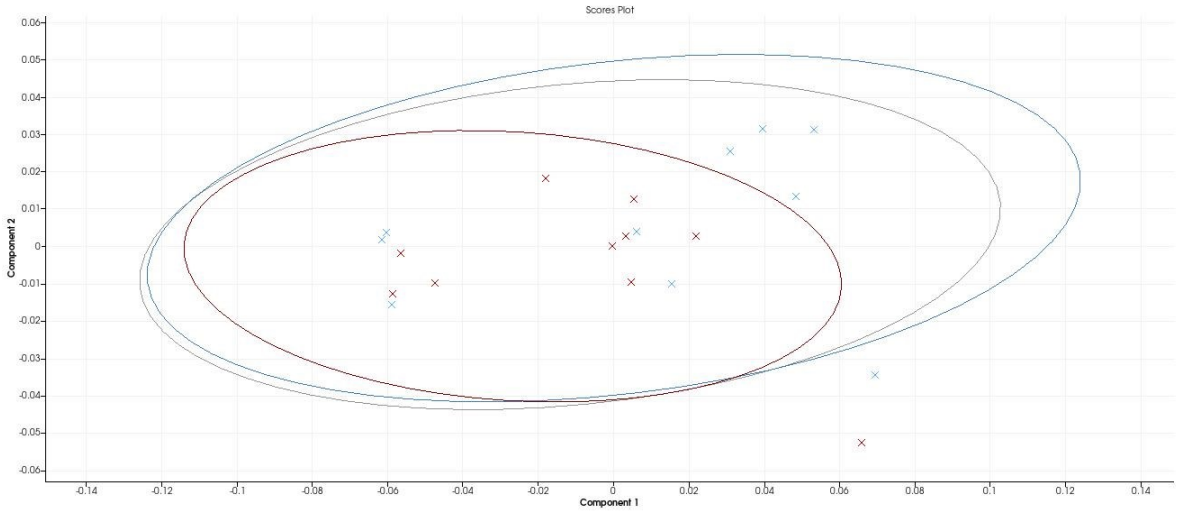

Image 13: PCA Scoring plot between left striata lesion vs non-lesion striata 50 µm.

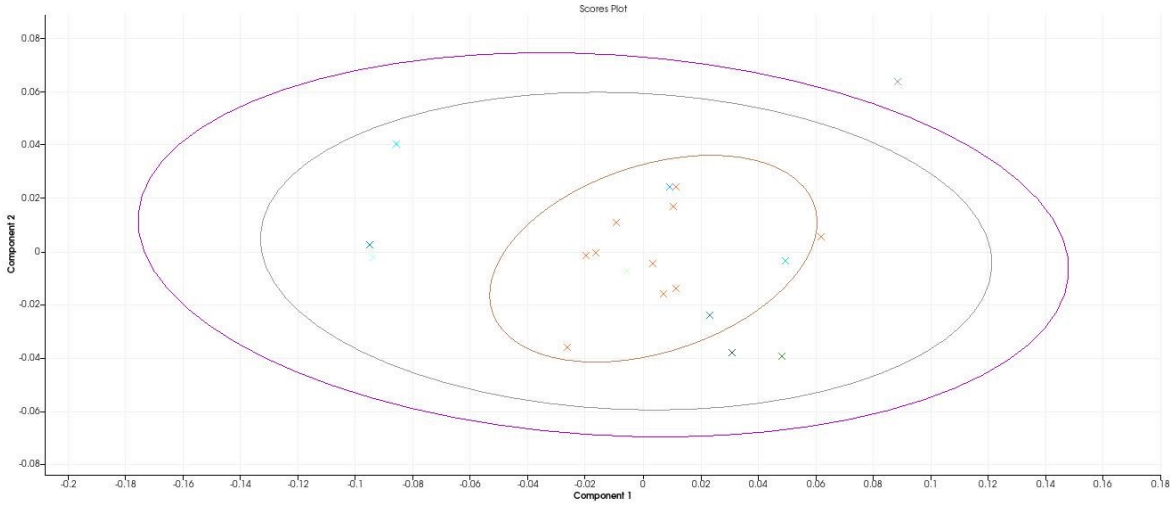

4.4 Results of hypothesis test and PCA loading scores

PCA loading values reflect the contribution of each ion (m/z feature) to the respective principal components. Higher absolute loading values indicate ions that drive the variance captured by that component, potentially distinguishing between lesioned and non-lesioned tissue regions. Positive and negative loadings correspond to differential ion intensities along the direction of separation defined by each principal component. Images 14 & 15 show how each of the 70 lipids contributes to the trend of the data. The lipids with a higher score contribute most to the trends within lesioned animals (Image 14) and between experimental groups (Image 15). The loading values per lipid are not as marked outside the software. In Table 3, the loading scores per lipid are noted, with the larger PCA component contributors marked red.

Image 14: PCA Loading plots between lesion striata vs control

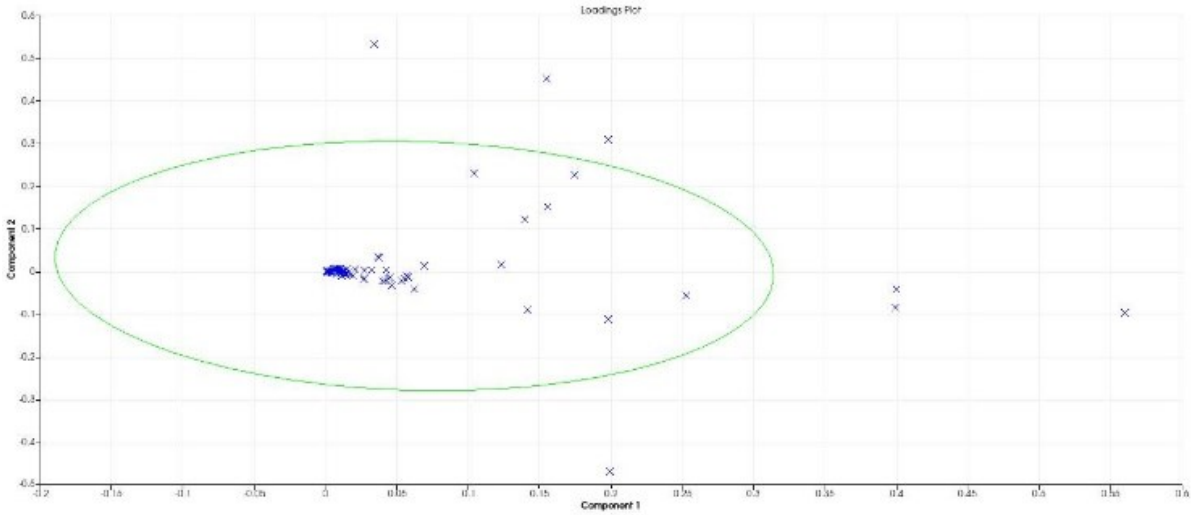

Image 15: PCA Loading plots within lesioned mice left (lesion) vs right (contralateral) striata.

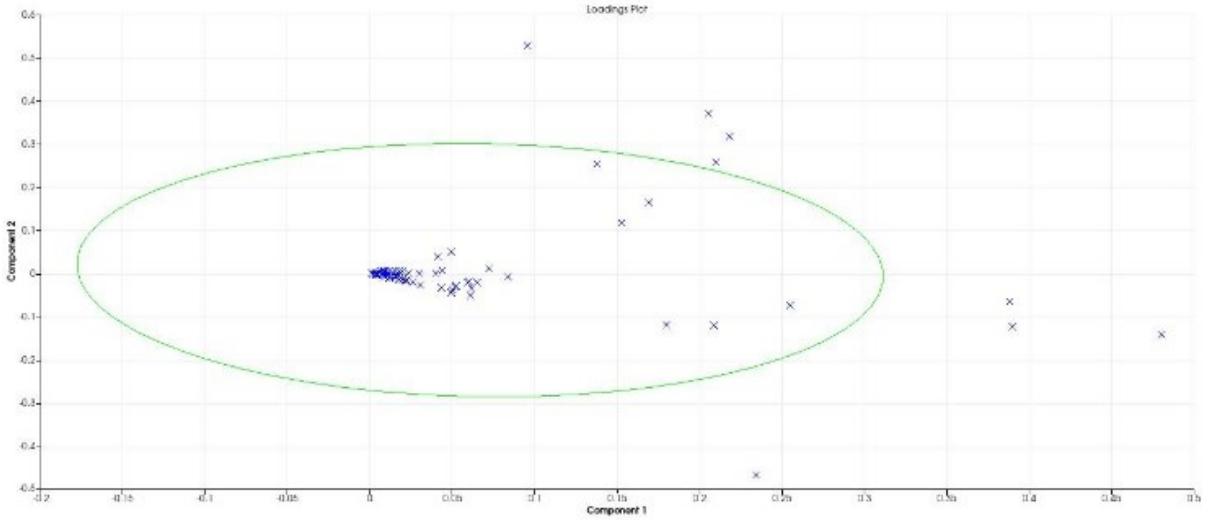

Table 3: Feature table of detected ionized lipids by MSI, including corresponding Kruskal-Wallis corrected p-values for group comparisons and PCA loading scores per lipid.

Ions	Kruskal-Wallis Corrected p-Value			PCA Loading scores	
m/z	All lesion vs sham between	Left Lesion vs Sham between	L vs R lesion within	L vs R within lesioned Loading 1	Left striata between groups Loading 1
768.5866	**0.0034**	**0.0409**	**0.0325**	0.065	0.053
758.5669	**0.0034**	**0.0409**	**0.0325**	0.015	0.014
774.5985	**0.0034**	**0.0409**	0.1287	0.055	0.057
806.5668	**0.0034**	**0.0409**	0.2987	0.010	0.011
746.567	**0.0034**	**0.0409**	0.5721	0.040	0.046
796.5819	**0.0153**	**0.0409**	0.6970	0.035	0.040
834.5977	**0.0153**	**0.0442**	0.6970	0.013	0.016
804.5495	**0.0432**	**0.0442**	0.1517	0.012	0.010
830.5621	0.0810	**0.0469**	0.1687	0.029	0.027
696.5814	0.0511	0.0597	0.4254	**0.357**	**0.400**
808.5799	**0.0467**	0.0758	0.5444	0.011	0.012
764.5198	0.1044	0.0959	0.6970	0.020	0.027
780.5869	0.1690	0.1207	0.5721	0.039	0.045
836.54	0.2439	0.1302	0.5612	0.015	0.019
698.5962	0.0667	0.1320	0.2954	**0.397**	**0.399**
768.5509	0.1690	0.1320	0.6970	0.009	0.010
700.6122	0.1461	0.1356	0.4099	**0.578**	**0.560**
752.5559	0.2996	0.1356	0.6025	0.017	0.017
652.5367	0.2314	0.1479	0.9648	0.016	0.027
588.5311	**0.0057**	0.1537	0.5444	**0.210**	**0.198**
578.5215	0.8526	0.1537	0.8063	0.066	0.062
728.5566	0.0511	0.1607	0.9209	0.041	0.042
782.5664	0.1526	0.1607	0.5630	0.002	0.002
792.5515	0.3812	0.1715	0.5444	0.005	0.007
856.5801	0.3812	0.1715	0.8888	0.025	0.021
776.557	0.3977	0.1715	0.5612	0.009	0.010
748.5248	0.3977	0.1715	0.6025	0.012	0.014
828.5514	0.5193	0.1715	0.7840	0.010	0.007
760.5837	0.0507	0.1880	0.7840	0.001	0.001
810.5979	0.1690	0.2056	0.6970	0.004	0.004
786.5992	0.0734	0.2176	0.5721	0.013	0.014
796.6337	0.5785	0.2176	0.4254	0.004	0.004

772.5238	0.2115	0.2374	0.5721	0.001	0.001
684.554	0.3638	0.2511	0.5444	0.237	0.252
830.5079	0.7688	0.2511	0.5444	0.015	0.010
826.5704	0.8285	0.3047	0.5630	0.003	0.002
524.371	0.6792	0.3211	0.6970	0.060	0.069
526.3335	0.7188	0.3211	0.6970	0.126	0.140
748.5825	0.5785	0.3384	0.1238	0.067	0.057
864.6961	0.7937	0.3384	0.2987	0.007	0.009
496.3387	0.1690	0.3652	0.1238	0.049	0.042
824.5546	0.9210	0.3933	0.8063	0.009	0.007
746.6037	0.1526	0.4039	0.1382	0.068	0.055
566.5491	0.3977	0.4039	0.5444	0.259	0.199
798.5395	0.8285	0.4039	0.5612	0.001	0.001
604.5049	0.7437	0.4243	0.8063	0.196	0.123
872.5545	0.7937	0.4243	0.5630	0.009	0.007
784.5805	0.9210	0.4860	0.5444	0.008	0.006
844.5236	0.9762	0.4860	0.7619	0.008	0.006
522.3568	0.1333	0.5410	0.9209	0.052	0.011
770.5075	0.6792	0.5410	0.6970	0.015	0.010
524.3213	0.9762	0.5410	0.6518	0.093	0.155
820.5237	0.7688	0.5641	0.8063	0.005	0.004
814.5313	0.8040	0.5641	0.6970	0.018	0.014
648.6267	0.3977	0.6327	0.7840	0.153	0.141
846.536	0.9560	0.6327	0.8414	0.011	0.009
534.2945	0.7437	0.6679	0.5630	0.055	0.036
788.6147	0.3977	0.6800	0.8414	0.004	0.004
540.3161	0.6024	0.6800	0.6025	0.010	0.034
510.2689	0.9210	0.6800	0.9648	0.107	0.104
548.3211	0.8040	0.7504	0.9209	0.138	0.174
734.568	0.8526	0.7504	0.6970	0.002	0.001
724.4954	0.5785	0.7857	0.6970	0.051	0.037
838.6284	0.3977	0.8693	0.6518	0.039	0.032
796.5236	0.2439	0.8979	0.5444	0.020	0.012
756.55	0.6024	0.8979	0.7840	0.004	0.003
542.330	0.8902	0.8979	0.6970	0.156	0.198
730.5717	0.9210	0.8979	0.6970	0.041	0.044
762.5953	0.9210	0.8979	0.8888	0.005	0.003
566.3309	0.8040	0.9769	0.8414	0.149	0.155

4.5 Selection and verification of lipids

A targeted list of 70 lipid species was assessed to investigate lipid distribution changes associated with brain lesions. These lipids were evaluated for differences in abundance between the lesion and contralateral hemisphere, as well as between the lesioned and sham-control group. Statistical testing using the Kruskal-Wallis (KW) method identified 9 lipids from the original 70 that showed significant differences (Table 3 &4). In addition, four more lipids that contributed largely to the PCA loadings and had (proximity to) statistical significance were selected: these show potential for biological relevance (Table 3 & 4). For these 13 total lipids, ion images were created to visualize spatial distribution patterns.

Since the lipids came pre-annotated within the SCiLS lab software, the molecular formulas corresponding to m/z were known with reasonable certainty in advance. To confirm correct identification, the theoretical monoisotopic mass of each compound was calculated based on its molecular formula using the following exact atomic masses:

Example Verification:

PC 40:6, $C_{48}H_{84}NO_8P$

C: 48 × 12.0000 = 576.0000

H: 84 × 1.0078 = 84.6552

N: 1 × 14.0031 = 14.0031

O: 8 × 15.9949 = 127.9592

P: 1 × 30.9738 = 30.9738

*Sum = **833.5913** + H^+ = **834.5986***

As an example, the lipid PC 40:6 ($C_{48}H_{84}NO_8P$) has a calculated monoisotopic mass of 833.5913 Da. After adding a proton (H^+), the expected m/z becomes 834.5986. The observed m/z in the experimental data was 834.5977, which matches the calculated value with high precision, confirming that the lipid was correctly annotated. Each of the 70 lipids was confirmed to be correctly annotated by providing the above instructions for calculations to AI, and randomly checking some against imprecision.

To further ensure accuracy, the selected lipid species were checked for possible overlap due to isomerism or adduct formation. In mass spectrometry, lipids can form alternative ionised species called adducts, such as $[M+Na]^+$, $[M+K]^+$, or $[M+NH_4]^+$, depending on the ions present in the solvent or instrument. Without accounting for isomers, these forms can lead to misidentification

(Oliveira-Lima et al, 2019). One potential isomere pair has been identified, with similar chemical formula & ion distribution found, but not m/z value; these are the PE's 38:1.

To address this, all observed m/z values were compared systematically to a reference list of common adducts using a customised Excel-based tool available at the laboratory. This confirmed that no two lipids in the dataset had overlapping or ambiguous m/z values. Each lipid ion appeared at a distinct and unique m/z value, but one potential and no adduct forms overlapped with any other lipid species, ensuring the detected ions represent chemically distinct lipid molecules.

As mentioned before, several lipid species may share the same mass-to-charge ratio. Highlighting how structural validation is necessary in lipidomic studies. The chemical formula and lipid name were provided within the SCiLS lab software, without alternatives. Therefore, the two most significant features were checked against the Lipid Maps database to confirm reliability (Lipid Metabolites and Pathways Strategy). So, the two most significant features, m/z 768.5866 and 758.5669, were checked for possible differing lipid identities. For example, the ion at m/z 768.5866 could correspond to multiple lipid identities, including PC O-36:4 (C44H82NO7P), PC 35:4 (C43H78NO8P), or PC O-35:5;O, all detected as [M+H]+ ions with small delta differences in mass accuracy. Similarly, m/z 758.5669 may represent LPC 34:3;O, PC 34:2, PC O-34:3;O, PC 33:3;O, or PC O-35:2, again with nearly identical measured masses but differing structural compositions. This ambiguity underscores the importance of complementary techniques such as MS/MS or co-elution with standards to confirm the exact lipid species detected in mass spectrometry data. It is important to note that one m/z value may represent some or all of the listed lipids.

Table 4: The interesting lipid with molecular formulas and m/z values calculated and observed.

m/z (Observed/Calculated)	Lipid Name	Chemical Formula	Contribution Type
768.5866	PC O-34:1	C42H84NO7P	Significant *** slight PCA
758.5669	PC 34:2	C42H80NO8P	Significant ***
774.5985	PE 38:1	C43H84NO8P	Significant ** slight PCA
806.5668	PC 38:6	C46H80NO8P	Significant **
746.567	PE 36:1	C41H80NO8P	Significant **
796.5819	PE 38:1	C43H84NO8P	Significant **
834.5977	PC 40:6	C48H84NO8P	Significant **
804.5495	PC 36:4	C44H80NO8P	Significant **
830.5621	PC 38:5	C46H82NO8P	Significant *
808.5799	PC 38:5	C46H82NO8P	Significant *
588.5311	Cer 36:1	C36H71NO3	Significant * + PCA

696.5814	DG O-42:8	C45H74O4	Near significance, PCA
700.6122	DG O-42:6	C45H78O4	PCA
698.5962	DG O-42:7	C45H76O4	Near significance + PCA

4.6 Visualization of Ionized lipids and linking to literature

This lipidomic analysis identified several lipid classes with statistical elevations and or large contribution to PCA, suggesting relevance in neuroinflammatory conditions like MS. Per class interpretation with a focus on lipids with significance or contribution to PCA variance is elaborated upon. Table 4 shows the lipids to be discussed in detail due to significance and or large PCA loading contribution; the lipid groups are PC, PE, ceramides, and DG. Per lipid, a Receiver Operating Characteristic (ROC) curve is included, showing the Area Under the Curve (AUC). The AUC indicates whether the data is no better than random (0.5), between 0.5-1.0 indicates better than random, and an AUC classifier < 0.5 indicates worse than random. A boxplot per lipid of lesioned tissue number 44 is included, comparing the abundance of the lipid in the drawn striatal lesioned versus the contralateral striatal area.

4.6.1 Ceramides

The Ceramide with m/z value of 588.5311 depicted below shows increased levels around the heart of the lesion (Image 16). Ceramides are bioactive lipids involved in inflammation, oxidative stress, and apoptosis. Cer (36:1) (m/z 588.5311) was found to be significant (* level) and contributed to PCA (0.210) variance, aligning with literature that implicates ceramide accumulation in neurodegenerative diseases and lesion development in MS (Ghorbani & Yong, 2021). Its presence in both near statistical and multivariate dimensions underscores its biological relevance, likely reflecting early-stage cell death or membrane breakdown.

Images 16: Lipid with m/z value 588.5311

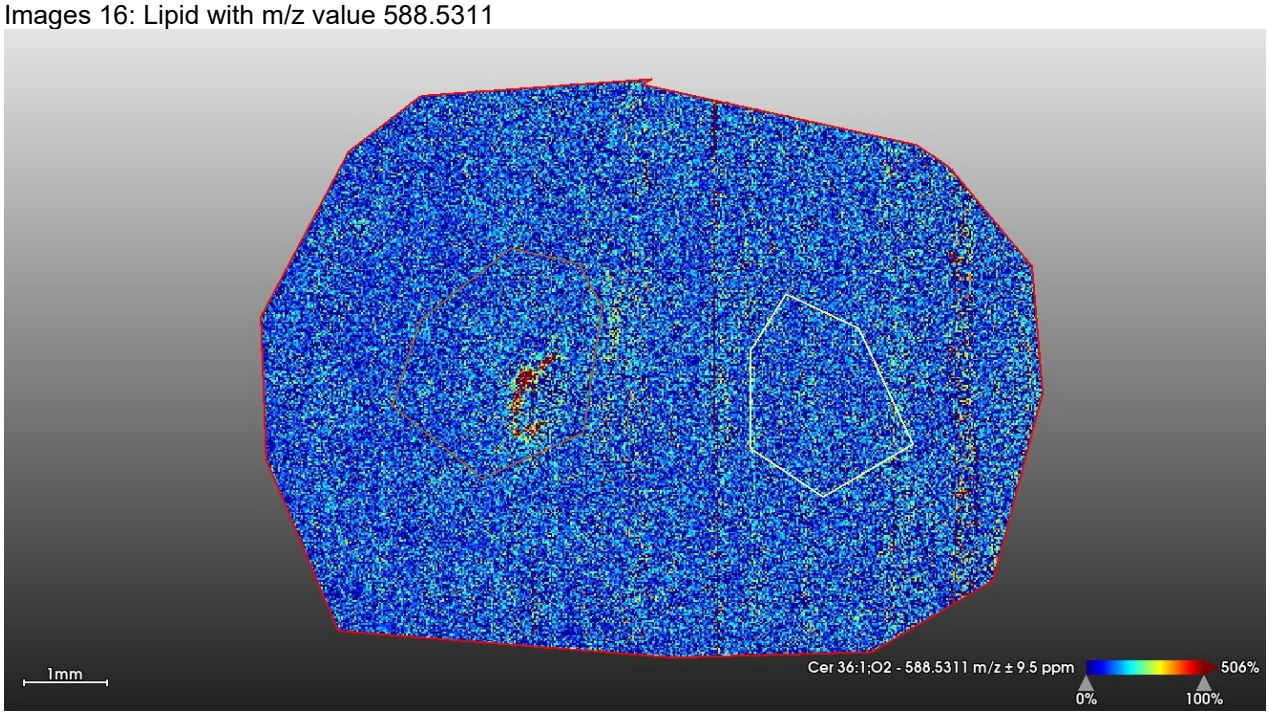

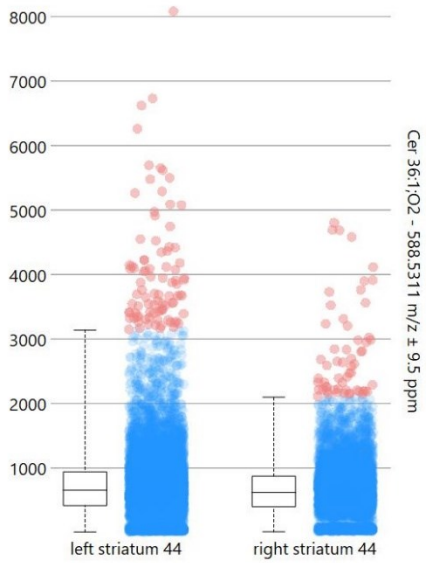

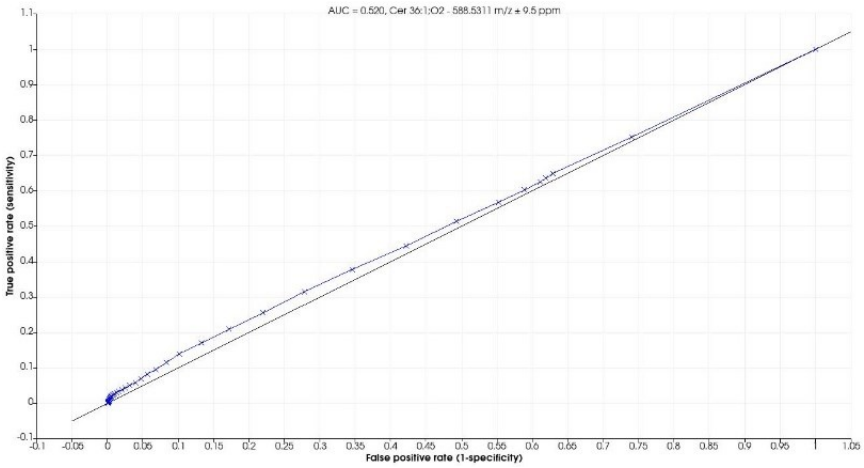

4.6.2 Phosphatidylcholines (PCs)

Phosphatidylcholines play essential roles in cell membrane integrity and inflammatory signalling (Del Boccio et al., 2011). Several phosphatidylcholine species exhibited strong statistical significance across lesion comparisons. These findings support the role of PC dysregulation in neuroinflammatory remodelling, consistent with prior observations in MS-related biofluids and CNS tissues (Ferreira et al., 2020; Razo et al., 2024). No LPC species reached significance in this dataset; however, LPCs are known to reflect phosphatidylcholine (PC) breakdown and are elevated during immune activation and demyelination. Altered LPC/PC ratios have been documented in MS patients (Cicalini et al., 2019). The PC species seemed to not only be concentrated around the lesion but also dispersed to the rest of the striatum and had lid up in the ventricles. This seems to be a trend for all significant PC species listed and depicted below (Images 17-22).

The following PC species were significantly altered:

- PC (34:2) (m/z 758.5669): *** significance; a major structural lipid, elevated in inflammatory contexts (Mallah et al., 2018).
- PC (36:4) (m/z 804.5495): ** significance; a polyunsaturated species possibly involved in oxidative stress response. In previous findings, PC 36:4 was linked to the lesion site but not in the rest of the brain, and it contributed to the PCA component (Mallah et al., 2018).
- PC (38:5) (m/z 830.5621): * significance; reported near MS lesions (Ferreira et al., 2020), though not specifically linked to neuroinflammation.
- PC (38:5) (m/z 808.5799): * significance; shares structural similarity with the above but lacks specific pathological linkage.
- PC (38:6) (m/z 806.5668): ** significance; a highly unsaturated lipid, potentially responsive to oxidative stress.
- PC (40:6) (m/z 834.5977): ** significance; a long-chain PUFA-containing species and strong PCA driver.
- PC(O-34:1) (m/z 768.5866): *** significance with slight PCA contribution; ether-linked PC, which have been associated with altered membrane signalling. Though this specific PC has not been observed as relevant to neuroinflammation before. (Sjövall et al., 2004)

Images 17: Lipid with m/z value 758.5670

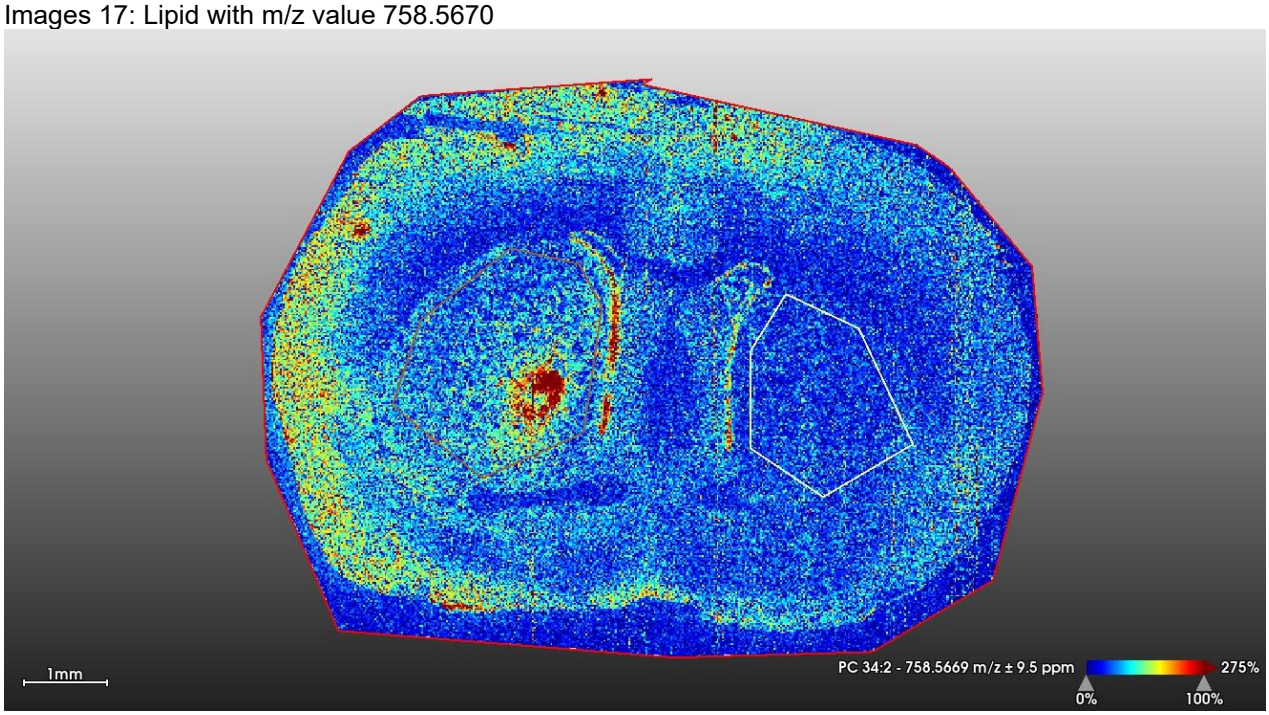

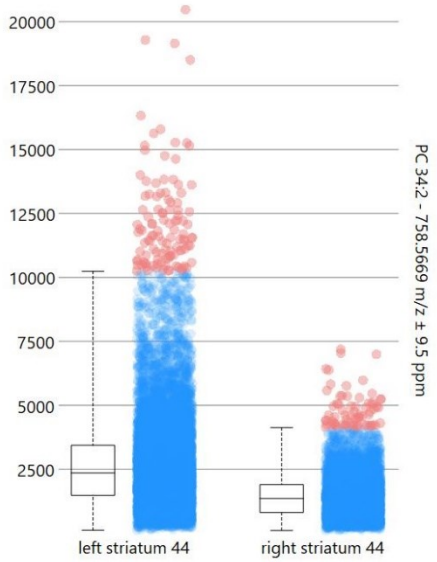

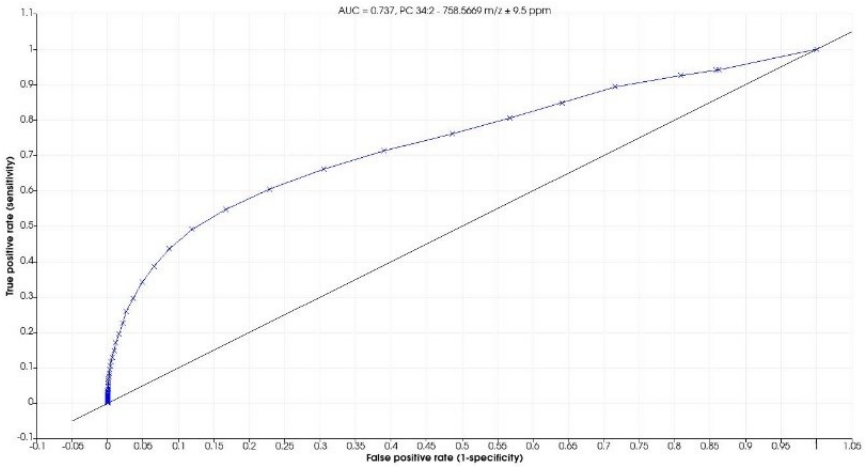

Description of lipid: This lipid was significant in all lesion vs sham (p = 0.0034***), left lesion vs sham (p = 0.0409*), and left vs right lesion (p = 0.0325*). PCA contribution was moderate. Likely PC (34:2), a core structural phosphatidylcholine elevated during neuroinflammatory and membrane remodelling. Its consistent statistical significance across contrasts supports its role in MS-related inflammation (Fereira et al, 2020).

Images 18: Lipid with m/z value 804.5495

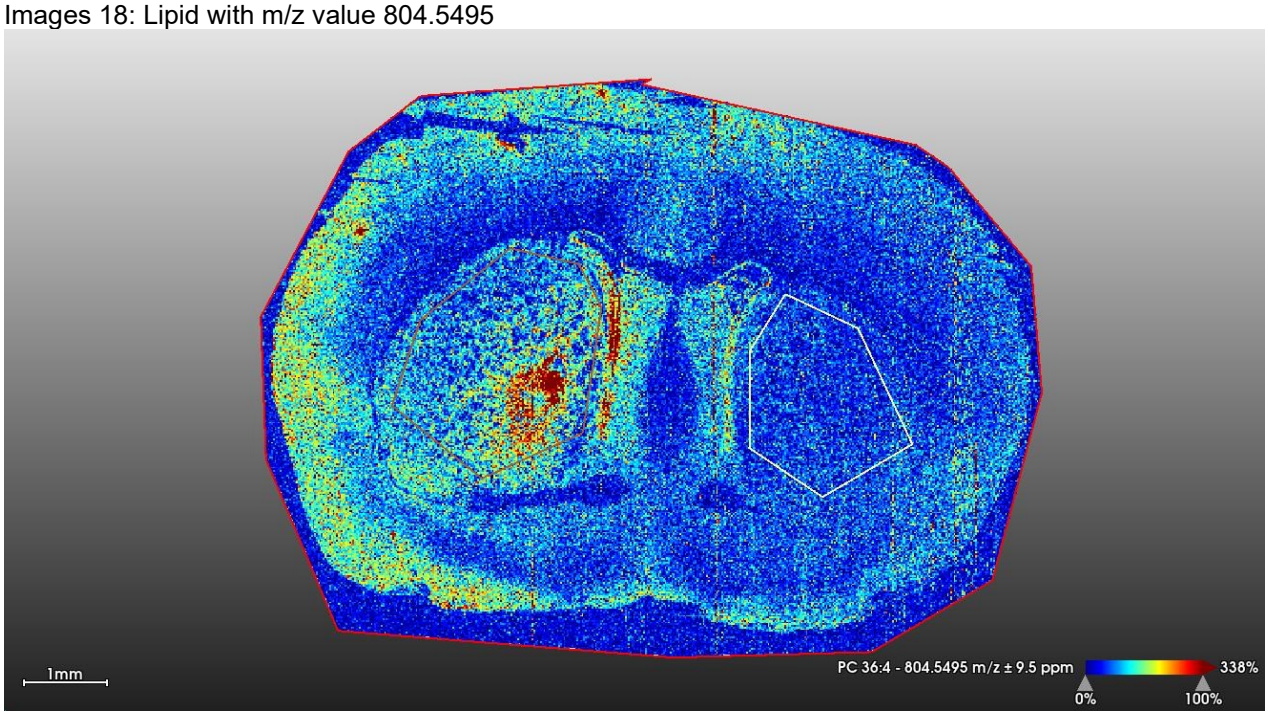

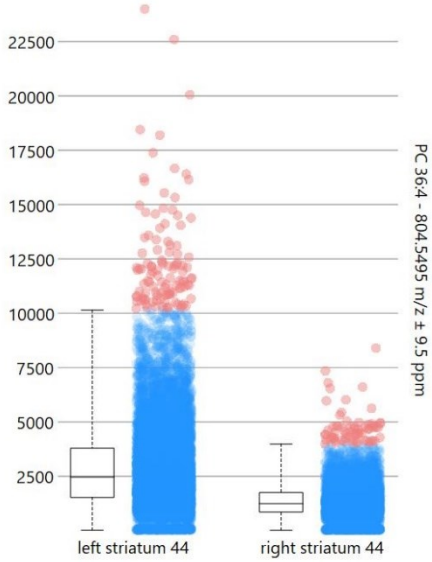

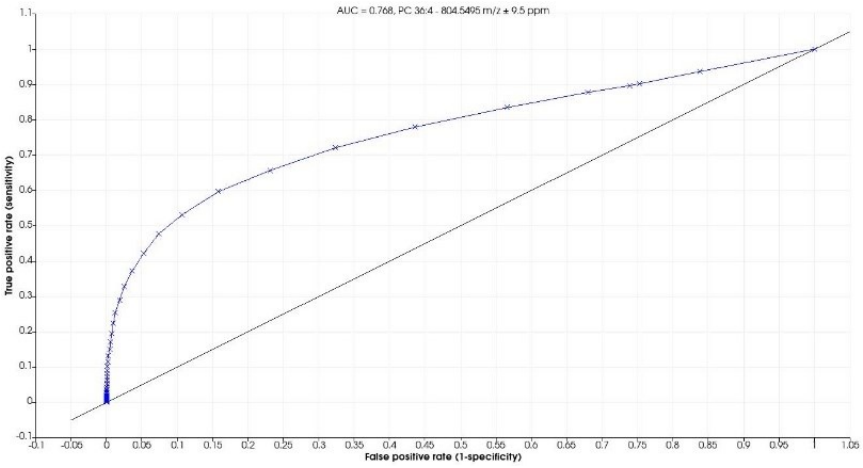

Description of lipid: This lipid was significant in all lesion vs sham (p = 0.0432*), and left lesion vs sham (p = 0.0442*), though not in lesion lateralization. The PCA contribution was modest. Likely PC (36:4), a polyunsaturated PC implicated in oxidative stress. Previously found enriched at lesion sites (Mallah et al., 2018), suggesting localized inflammatory membrane remodelling (Mallah et al., 2018).

Images 19: Lipid with m/z value 830.5621

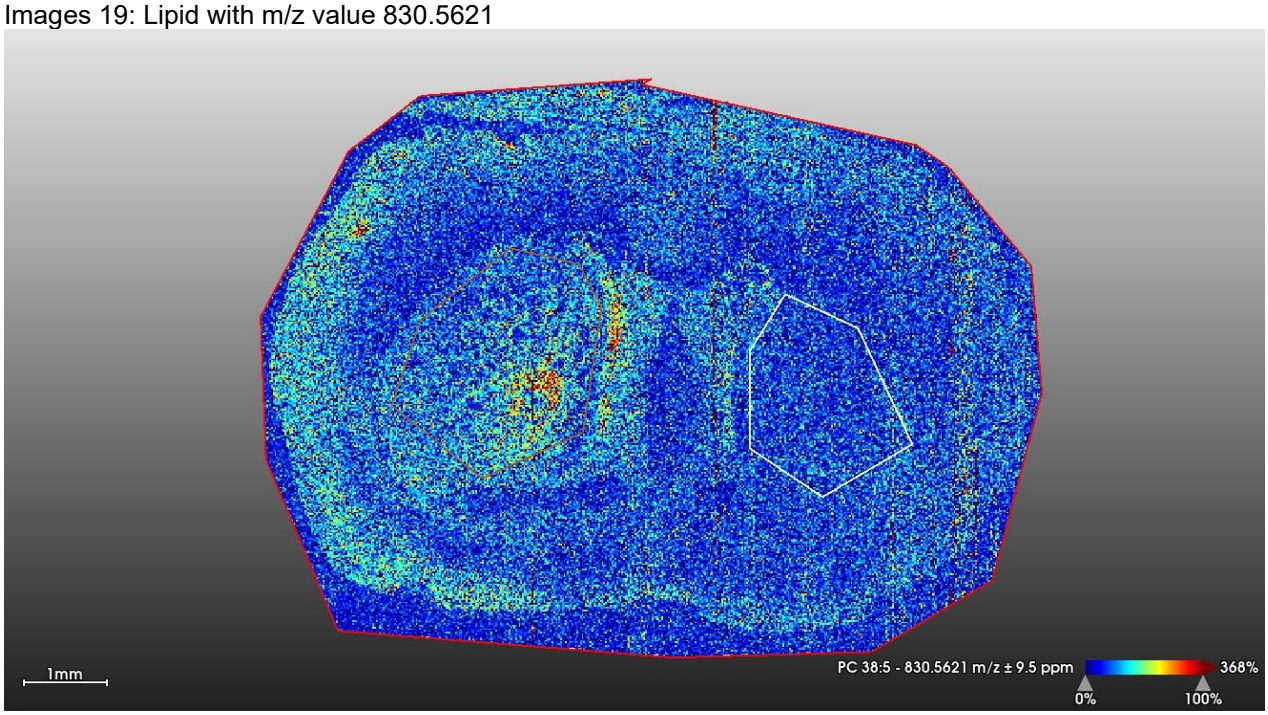

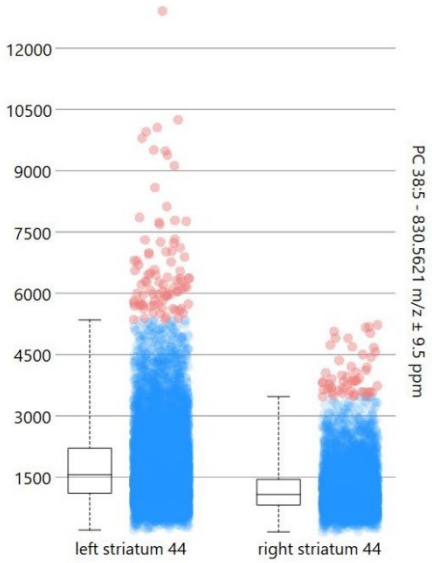

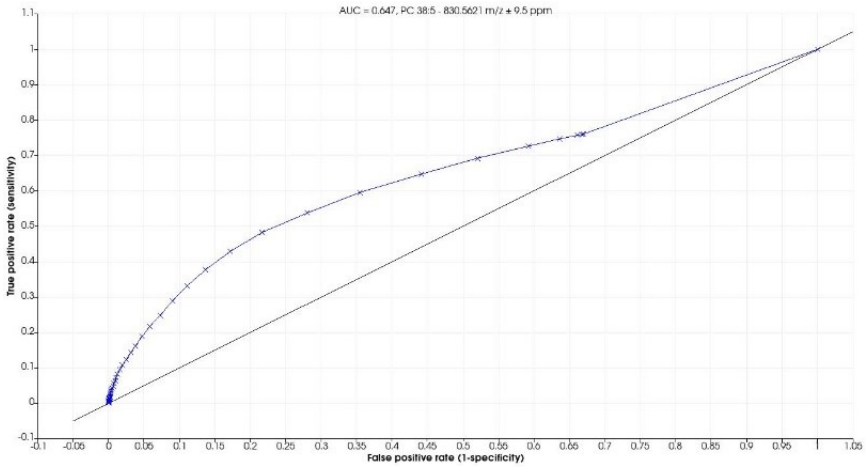

Description of lipid: This lipid was near-significant in left lesion vs sham (p = 0.0469*), with non-significant but trending values in all lesion vs sham (p = 0.0810) and left vs right lesion (p = 0.1687). PCA contribution was modest (2.9% within, 2.7% between). Likely PC (38:5), a PUFA-rich phosphatidylcholine, was reported near MS lesions (Ferreira et al., 2020). Suggests lateral sensitivity and involvement in lesion-induced demyelination.

Images 20: Lipid with m/z value 808.5799

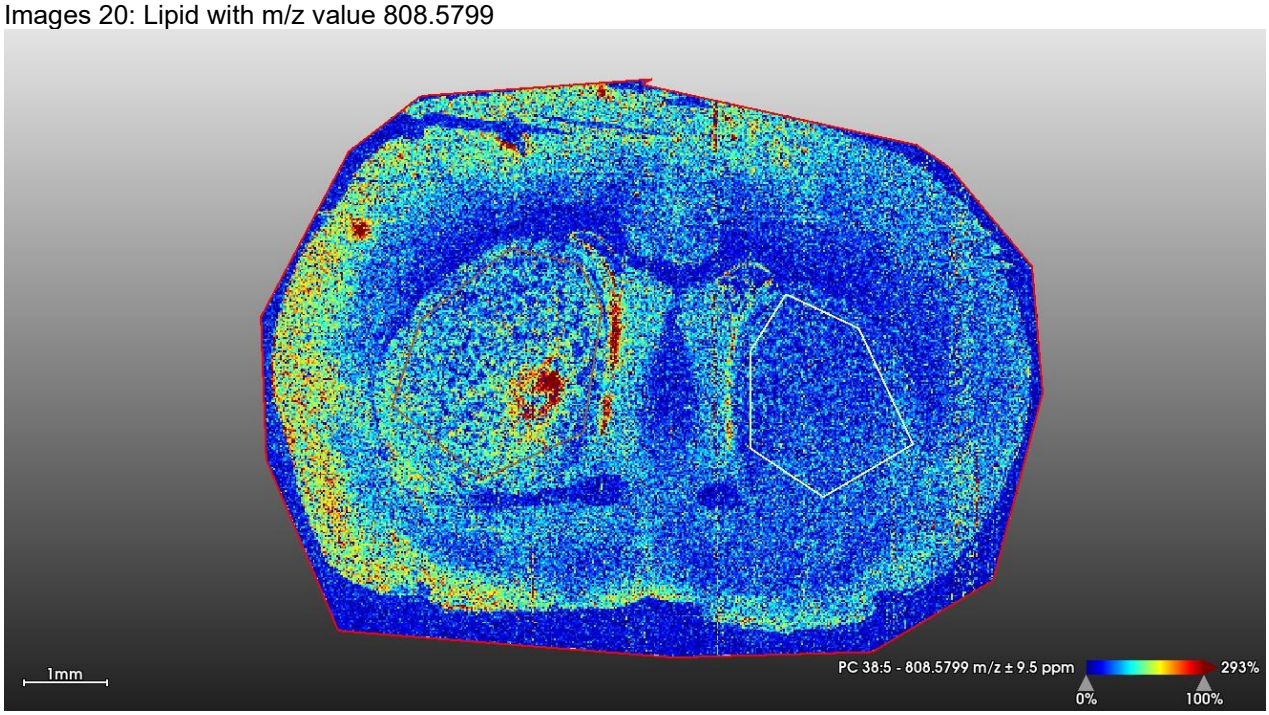

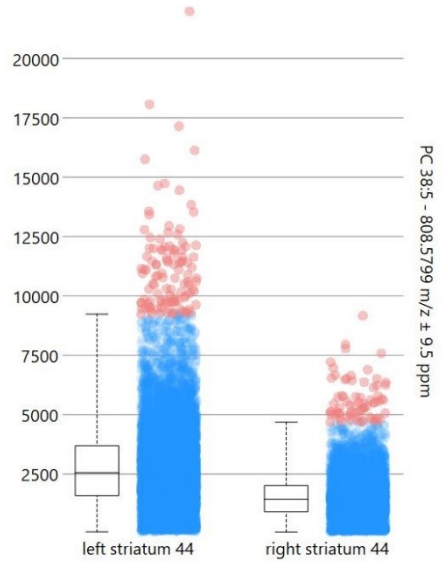

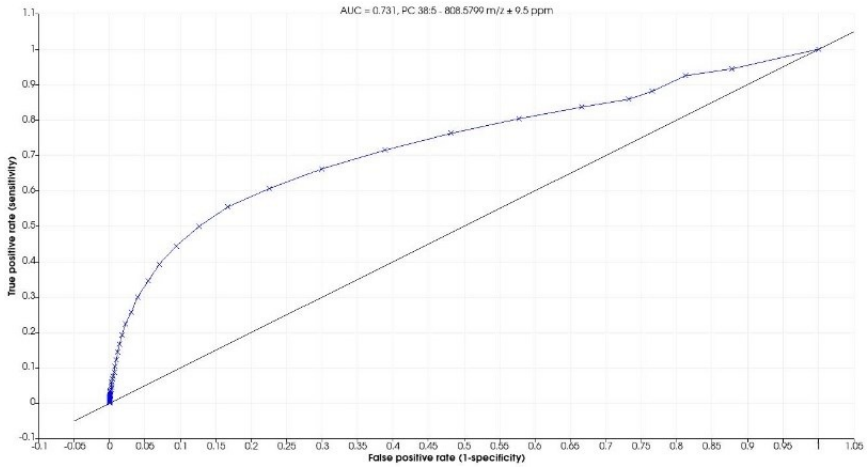

Description of lipid: This lipid was near-significant in all lesion vs sham (p = 0.0467*), though not significant in other contrasts. PCA contribution was low. Another isomer of PC (38:5), potentially reflecting overlapping metabolic pathways. Lacks a direct pathological link but may co-vary with lesion-associated PCs. The lipid shares structural similarities with the previous lipid (m/z 830.5621). Likely PC (38:5) (C46H82NO8P), involved in membrane stability and potentially related to neuroinflammation.

Images 21: Lipid with m/z value 806.5668.

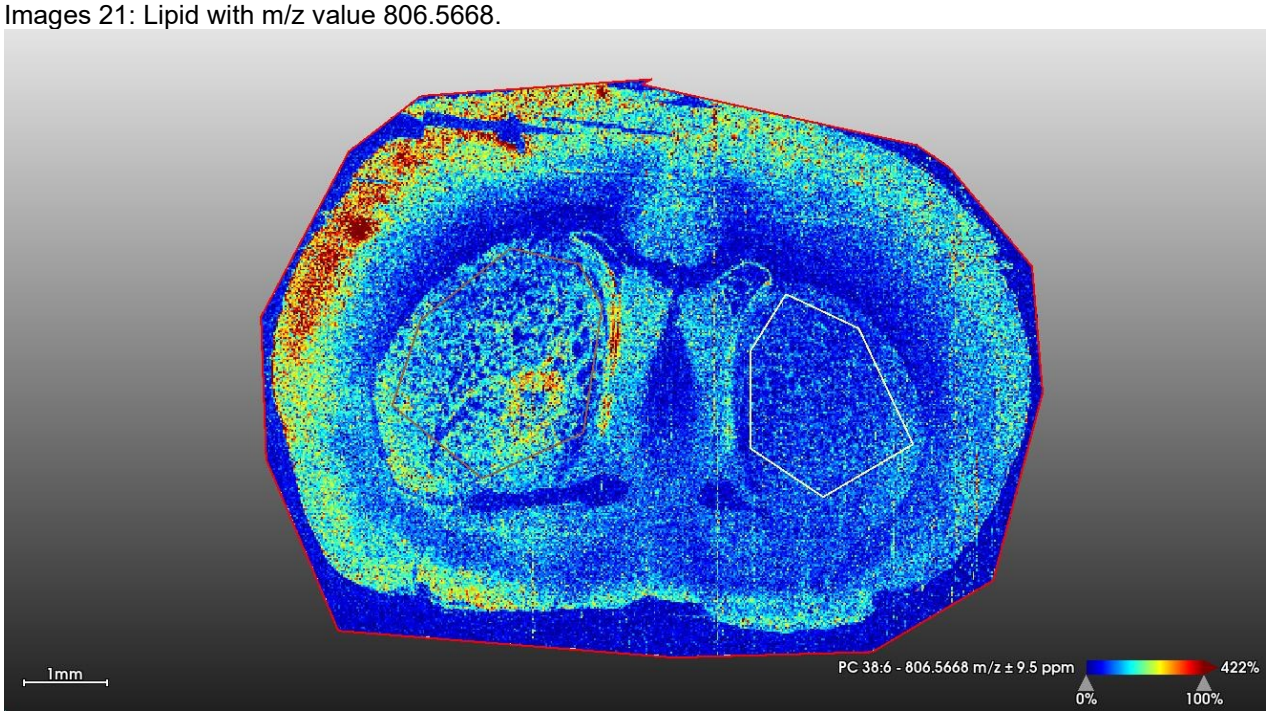

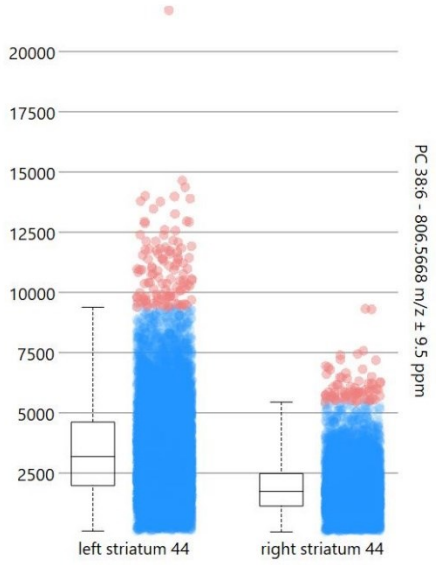

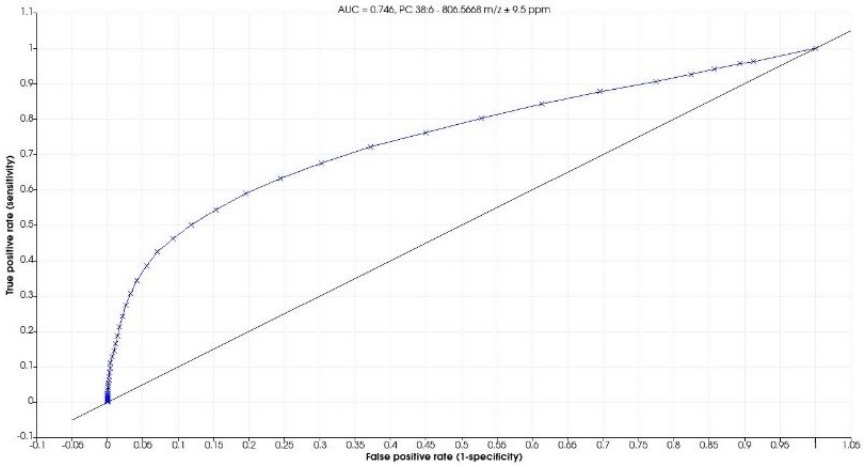

Description of lipid: This lipid was significant in all lesion vs sham (p = 0.0034**), and in left lesion vs sham (p = 0.0409*), though not significant in lateral comparisons. The PCA contribution was low. Likely PC (38:6).

Images 22: Lipid with m/z value 834.5977.

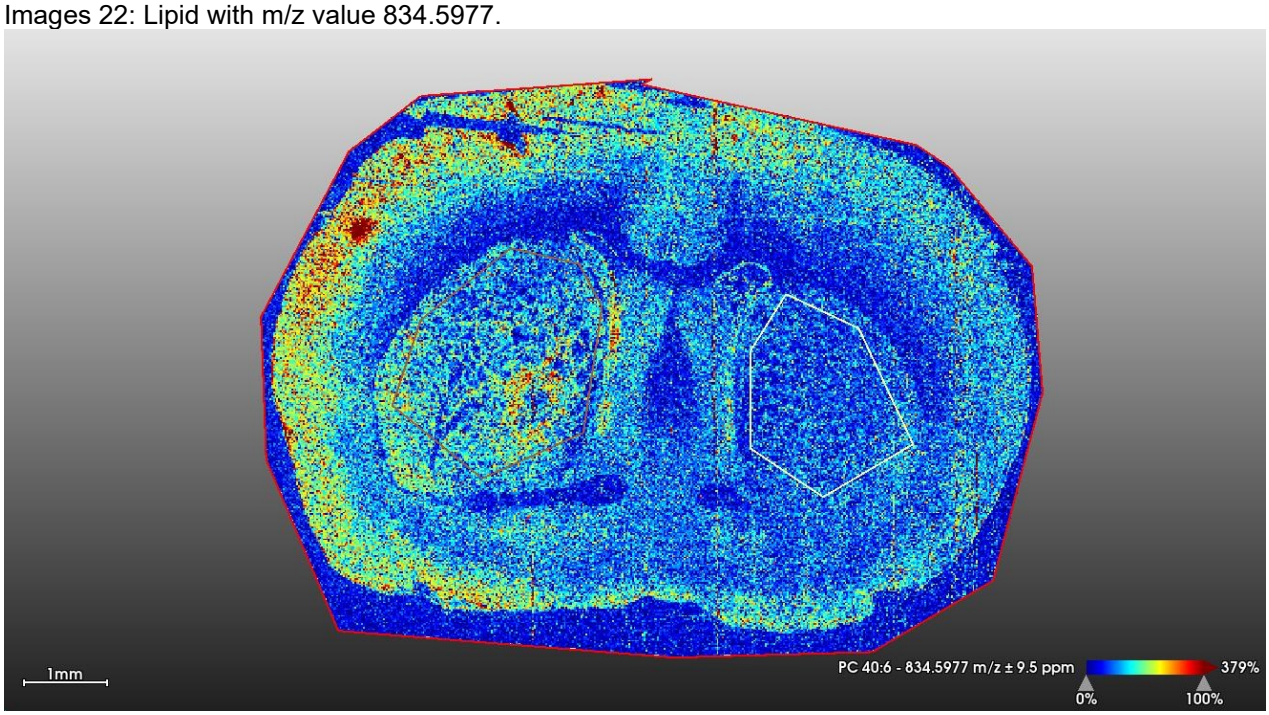

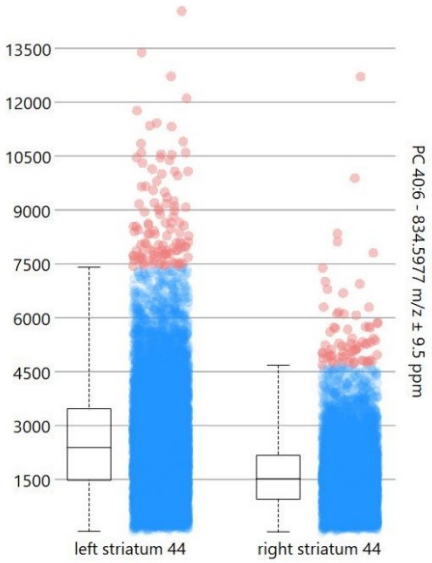

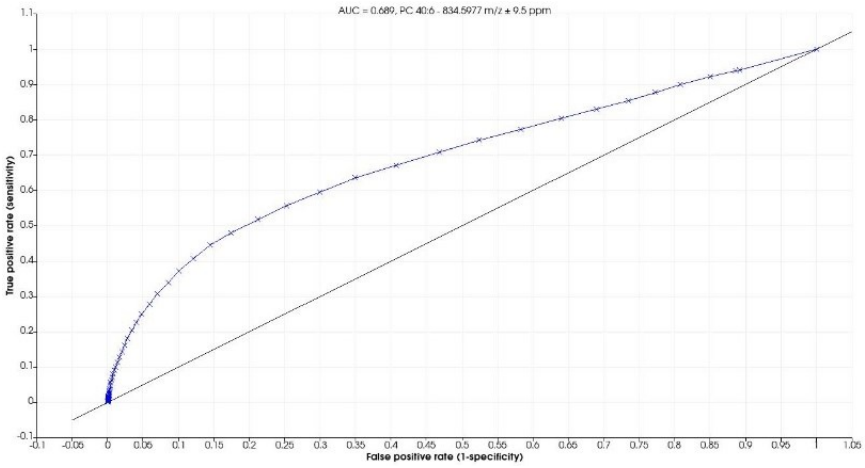

Description of lipid: This lipid was significant in all lesion vs sham (p = 0.0153*), and in left lesion vs sham (p = 0.0442*). PCA contribution was modest (1.3% within, 1.6% between). Likely PC (40:6), a long-chain PUFA species. Its presence aligns with increased lipid remodelling and membrane fluidity demands during neuroinflammation (Razo et al, 2024).

Images 23: Lipid with m/z value 768.5866.

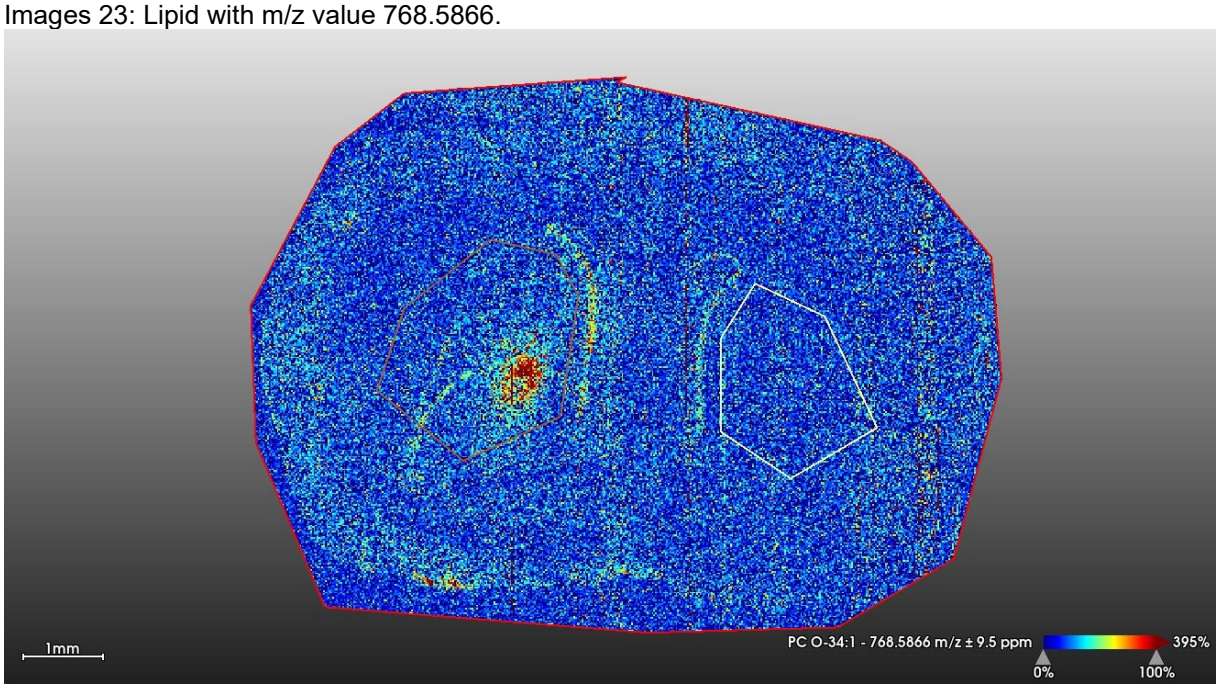

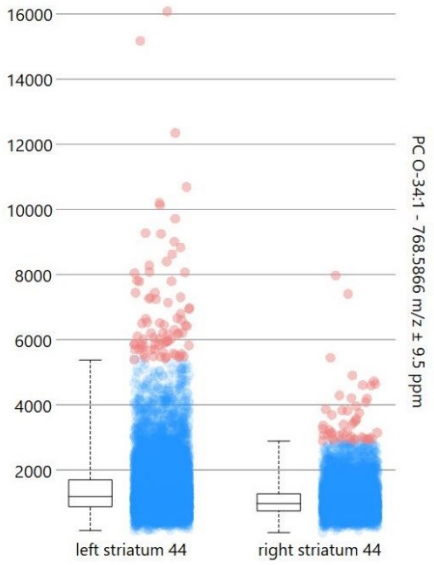

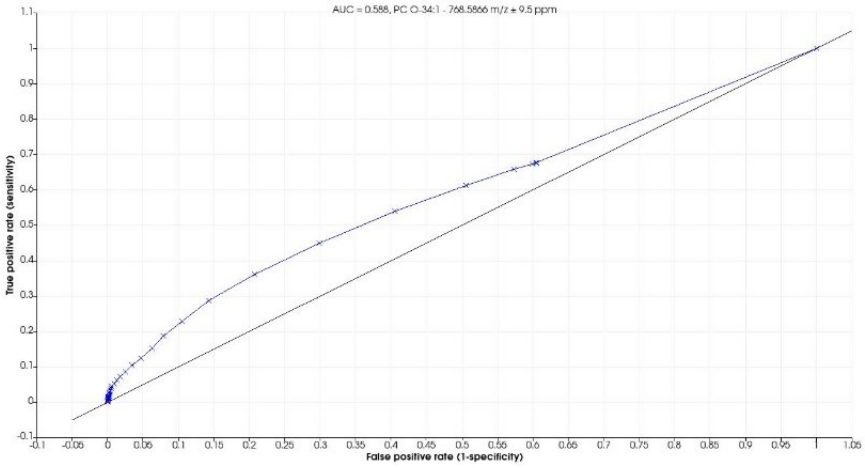

Description of lipid: This lipid was significant in all lesion vs sham (p = 0.0034***), in left lesion vs sham (p = 0.0409*), and in lesion lateralization (p = 0.0325*). PCA contribution was moderate. Likely PC O-34:1, an ether-linked phosphatidylcholine often associated with membrane signalling. Data supported by Sjövall et al. (2004), from which the images below originate. This PC is O-linked which could be the reason for its altered ion distribution compared to other PCs.

760.63	$C_{10}H_{19}O_8NP-C_{32}H_{64}^+$	PC 34:1
788.65	$C_{10}H_{19}O_8NP-C_{34}H_{68}^+$	PC 36:1

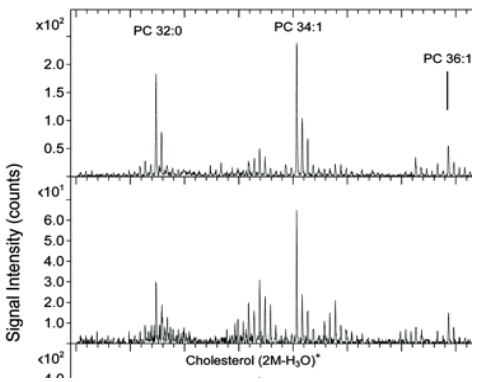

4.6.3 Phosphatidylethanolamines (PEs)

PEs are essential phospholipids contributing to membrane curvature and apoptotic signalling (Mallah et al., 2018). The following PE species were observed to be only slightly more concentrated in the lesioned left striatum:

- PE (36:1) (m/z 746.5670): ** significance; while PEs are broadly implicated in membrane dynamics and apoptosis, this specific lipid lacks a direct neuroinflammation link.
- PE (38:1) (m/z 774.5985 and 796.5819): ** significance; the former contributed slightly to PCA variance. PE dysregulation may reflect oxidative and inflammatory stress responses, though no direct MS or lesion-specific link was identified. A previous finding linked PE to the cortex region but not in the ventricles or surrounding lesions. (Mallah et al, 2018). These two lipids are potential isomers from each other.

Images 24: Lipid with m/z value 746.5670.

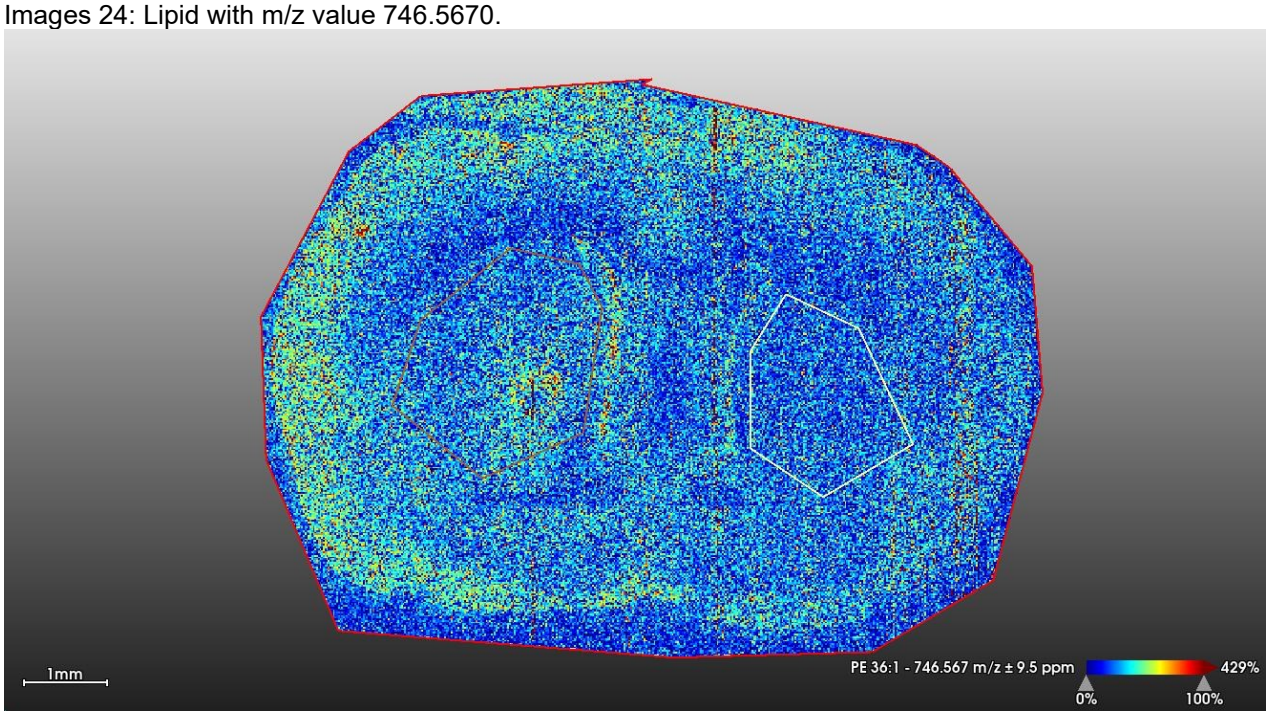

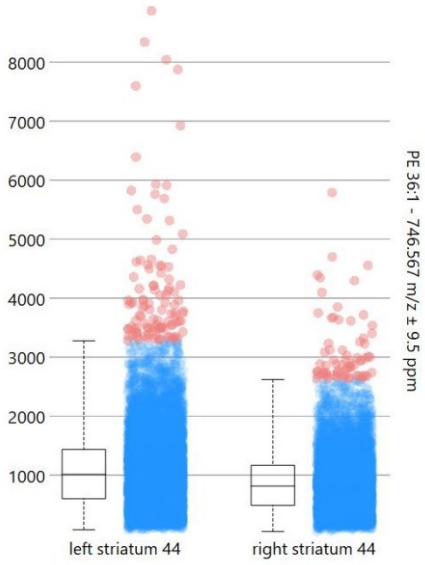

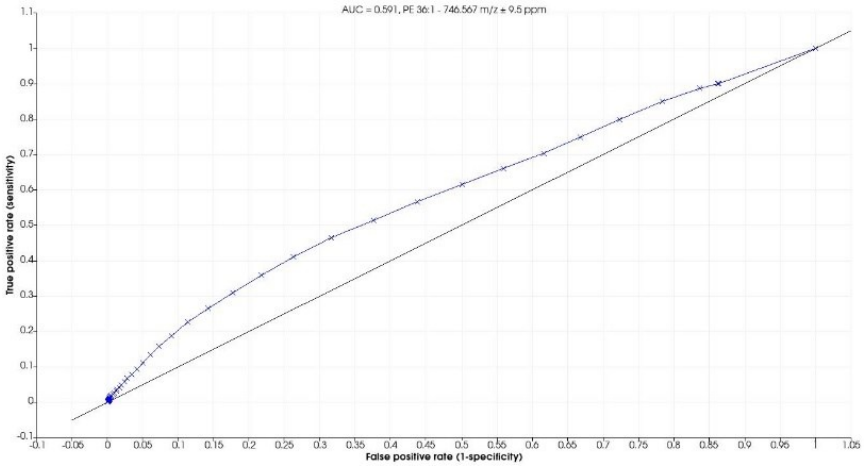

Description of lipid: This lipid was significant in all lesion vs sham (p = 0.0034**), and left lesion vs sham (p = 0.0409*), but not in lateral comparisons (p = 0.5721). PCA contribution was low. Likely PE (36:1), a monounsaturated PE species involved in shaping membrane curvature and apoptosis. While not directly linked to neuroinflammation, its altered levels may reflect broader membrane stress responses under pathological conditions (Mallah et al., 2018).

Images 25: Lipid with m/z value 774.5985.

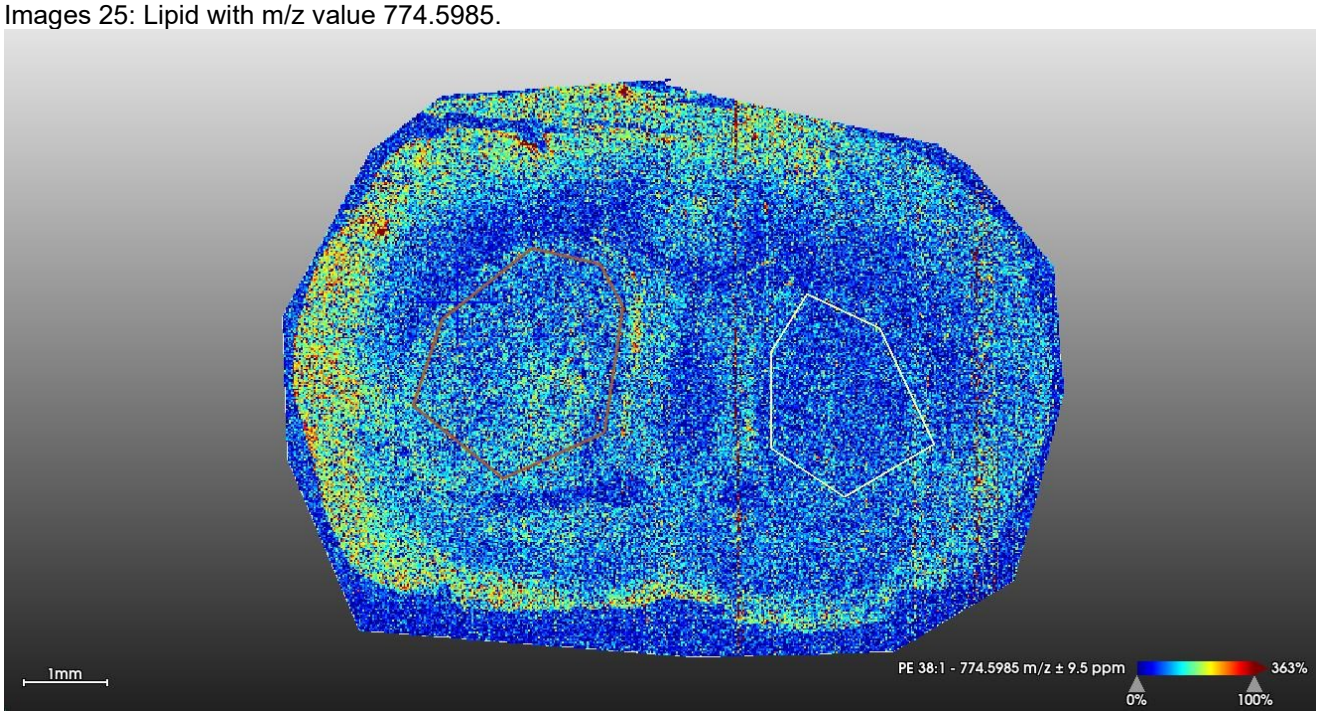

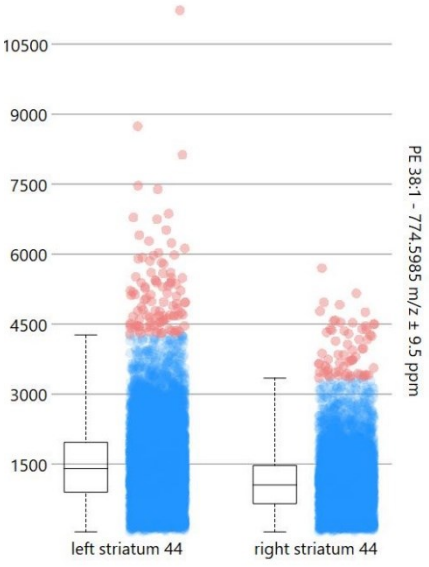

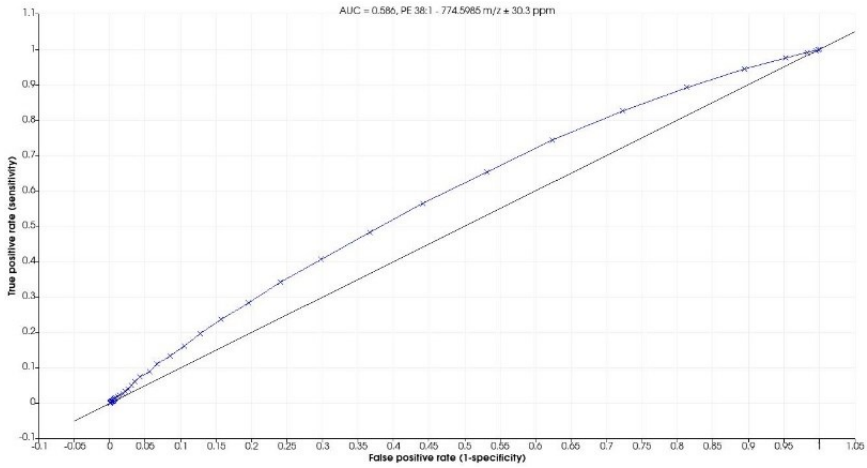

Description of lipid: This lipid was significant in all lesion vs sham (p = 0.0034**), and left lesion vs sham (p = 0.0409*), with non-significant p = 0.1287 for lateral comparisons. PCA contribution was moderate. Assigned as PE (38:1). It may reflect neuroinflammatory compensation in remote regions rather than at the lesion core, as this species has previously been linked to the contralateral cortex region but not the lesion site (Mallah et al., 2018).

Images 26: Lipid with m/z value 796.5819.

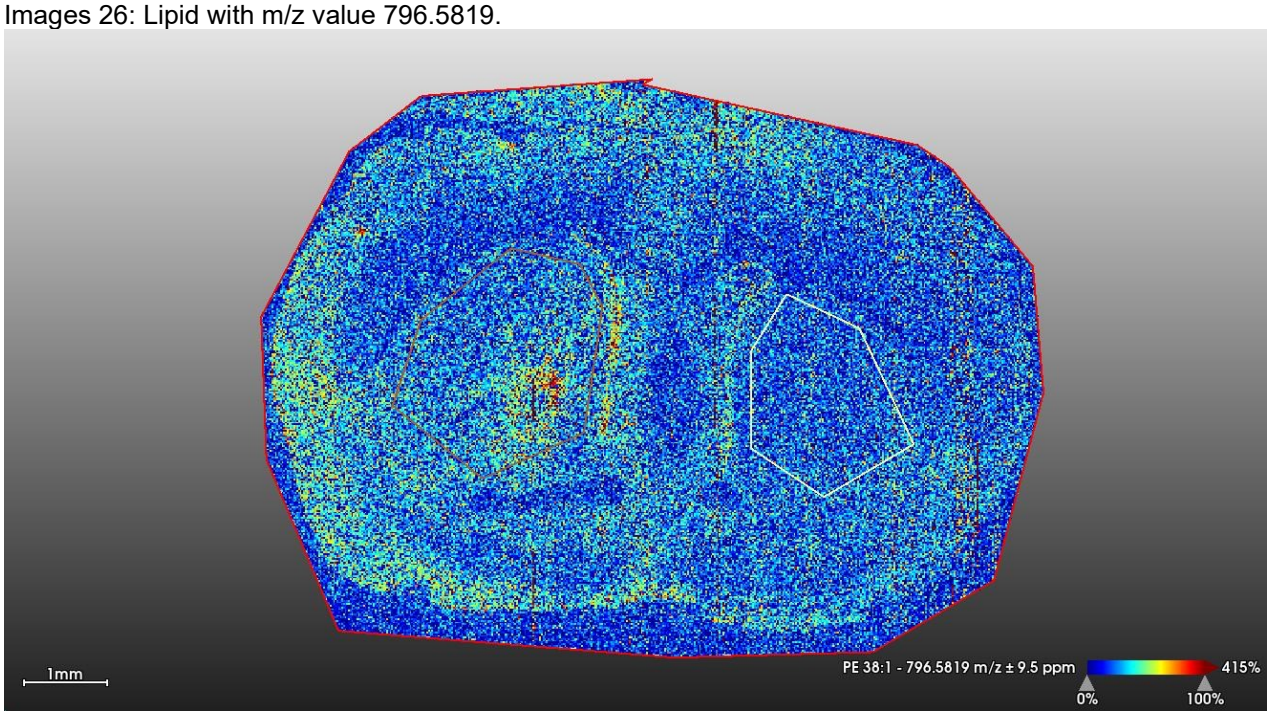

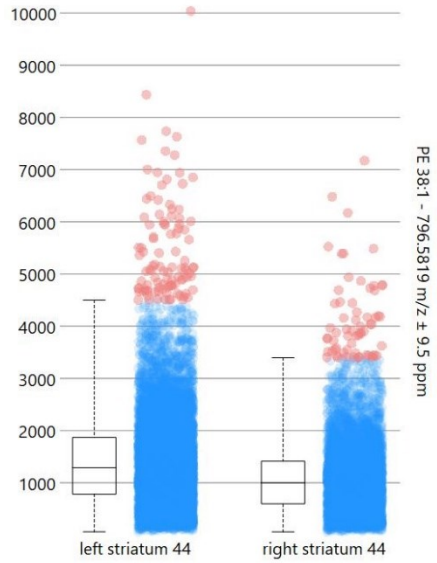

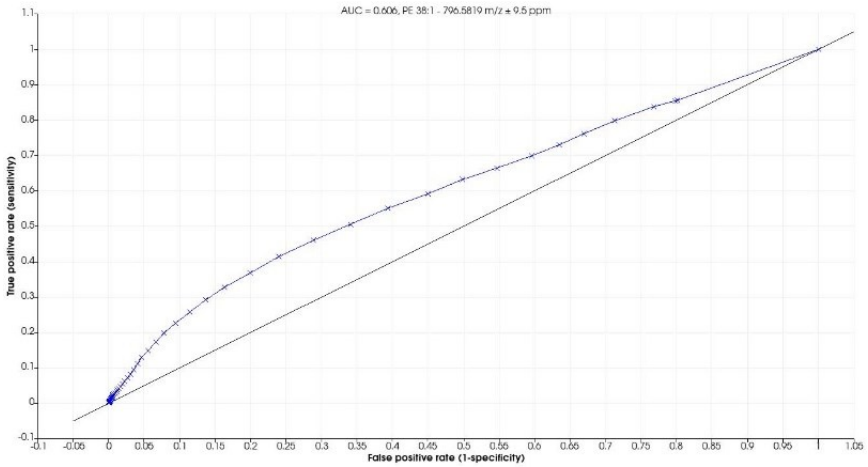

Description of lipid: *This lipid showed significance in all lesion vs sham (p = 0.0153*), and left lesion vs sham (p = 0.0409*), but not in lateral comparisons (p = 0.6970). PCA contributions were modest (3.5% within, 4.0% between). Also identified as PE (38:1) (likely isomeric). Structural similarity to 774.5985 supports a shared functional role in stress-related phospholipid remodelling (Mallah et al., 2018).*

4.6.4 Diglycerols (DGs)

DGs are signalling lipids involved in various cellular processes, including inflammation (Ferreira et al., 2020). DGs can be rapidly generated in response to inflammatory stimuli, activating downstream signalling cascades (Hansen & Wang, 2023). As a class, DGs are known to mediate inflammatory cascades, suggesting potential relevance in neuroinflammation (Ferreira et al., 2020). Elevated DGs can lead to increased oxidative stress (Hansen & Wang, 2023). These are PCA contributors, particularly within the left striata, but as these are insignificant, the trends must be validated further. From the ion images below, the DGs seem to have high intensity directly where the lesion is in the brain and a slight increase in the ventricle.

- DG O-42:6 (m/z 700.6122): PCA contributor; however, no specific literature linking this lipid to neuroinflammation could be found. This lipid had the highest PCA loading score of 0.578, suggesting a dominant contributor within the dataset, despite not differing between lesion and sham striata.
- DG O-42:7 (m/z 698.5962): Near significant with PCA contribution.
- DG O-42:8 (m/z 696.5814): Near significance with PCA; likely to be involved in similar signalling pathways due to structural homology. (Podbielska et al, 2021).

Images 27: lipid with m/z value 700.6122.

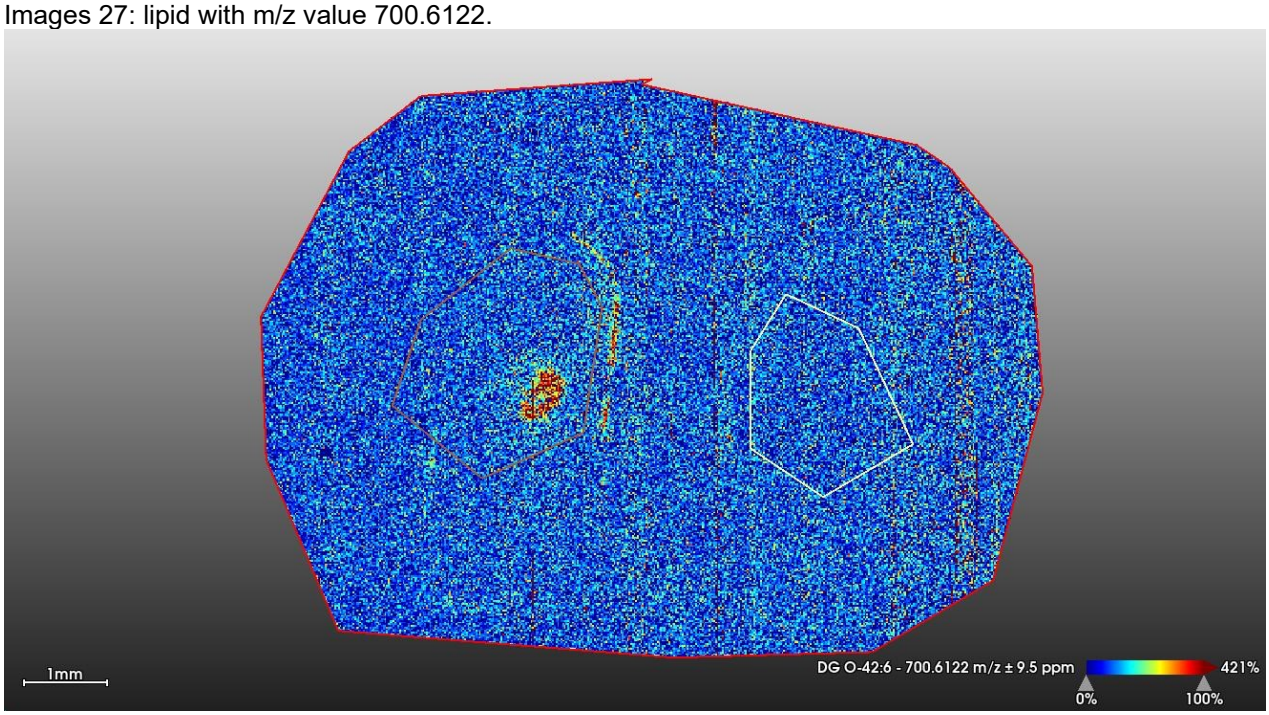

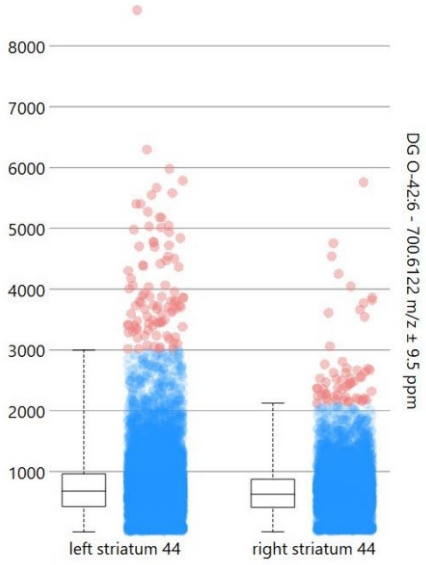

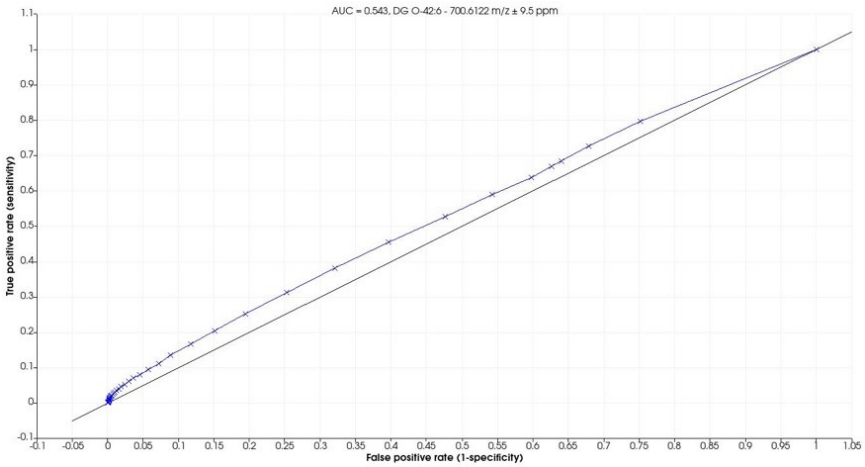

Description of lipid: This lipid showed no significant KW differences ($p > 0.13$), but had high PCA contribution (57.8% within, 56.0% between). Likely DG O-42:6, an ether-linked diacylglycerol. While no direct association with MS or CNS lesions has been found, its strong multivariate impact suggests functional relevance in lipid signalling within the lesion context

Images 28**:** lipid with m/z value 698.5962.

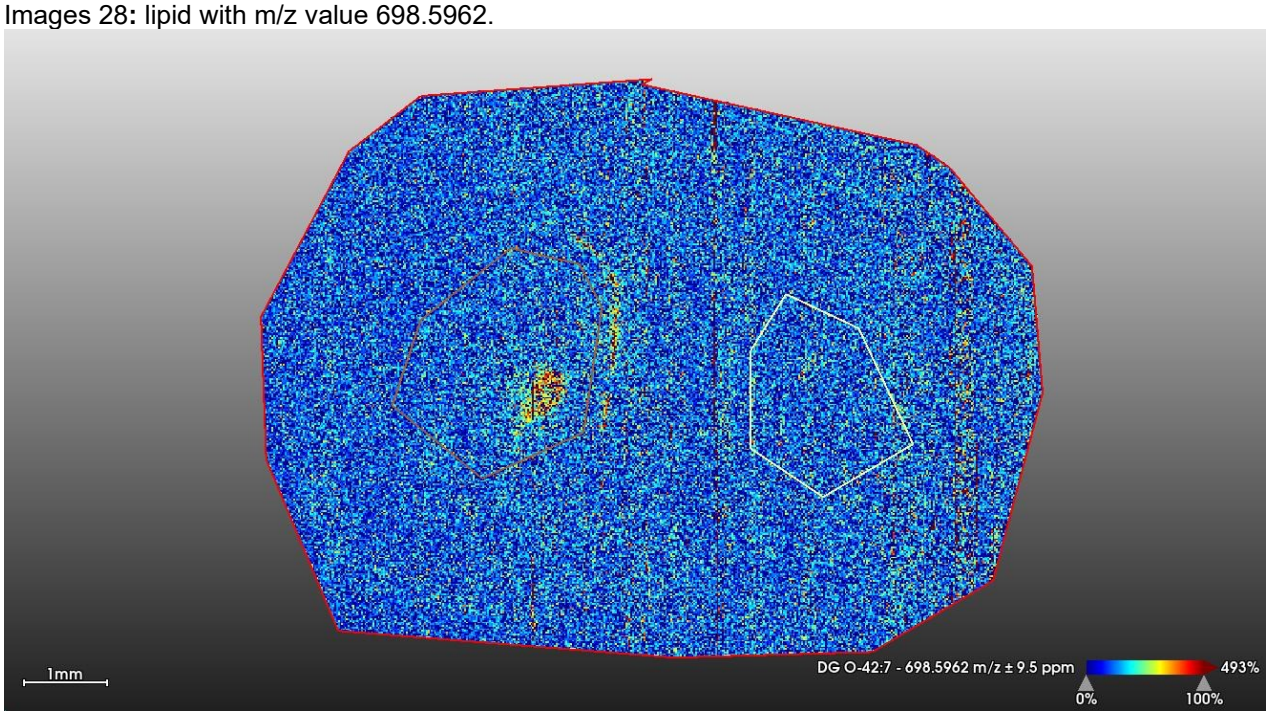

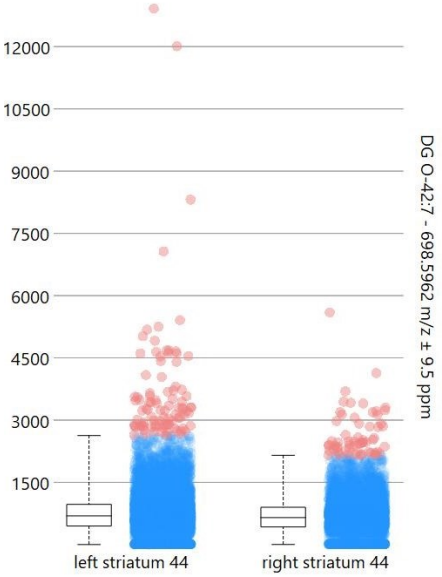

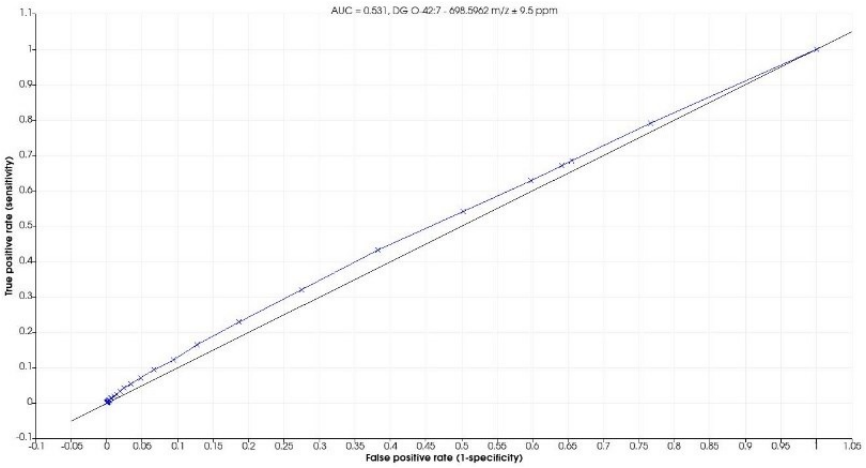

Description of lipid: This lipid was near-significant in all lesion vs sham (p = 0.0667), with strong PCA contribution (39.7% within, 39.9% between). Assigned as DG O-42:7, this ether-linked species is structurally homologous to other DGs in inflammatory cascades. Given DGs' known roles in activating PKC and modulating immune responses, this lipid may have a non-random role in lesion-associated remodelling (Ferreira et al, 2020).

Images 29: lipid with m/z value 696.5814

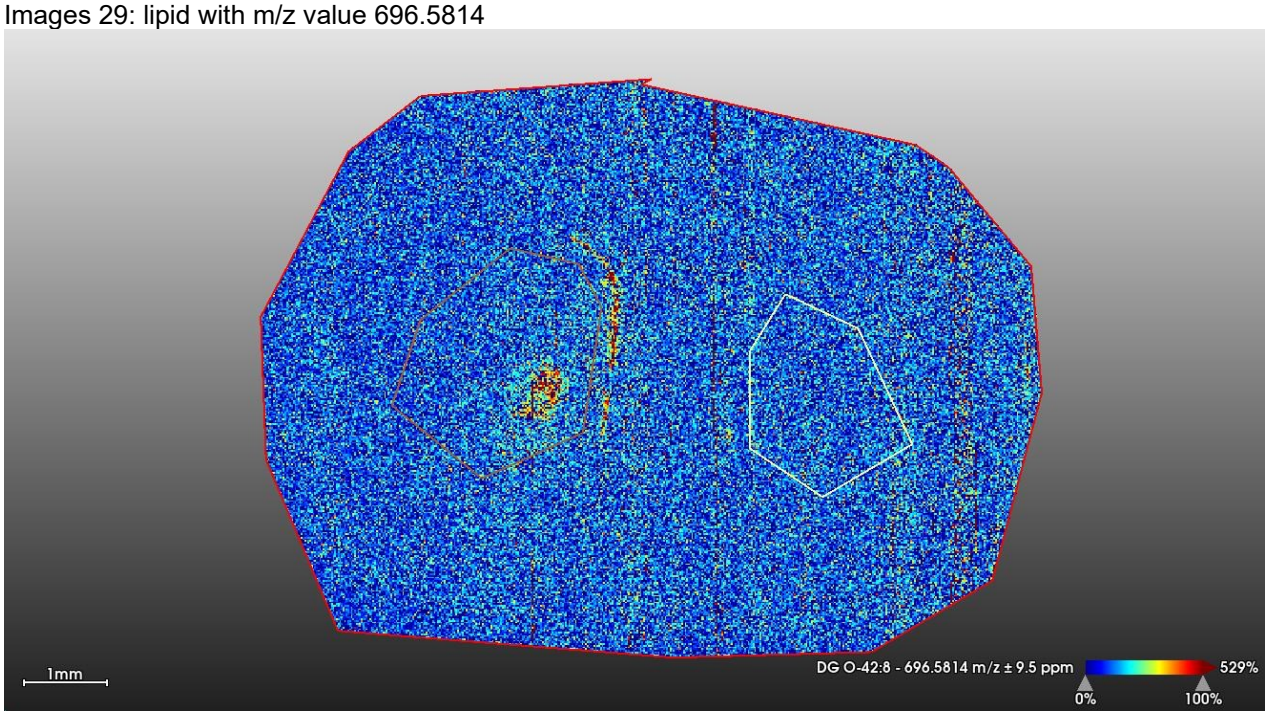

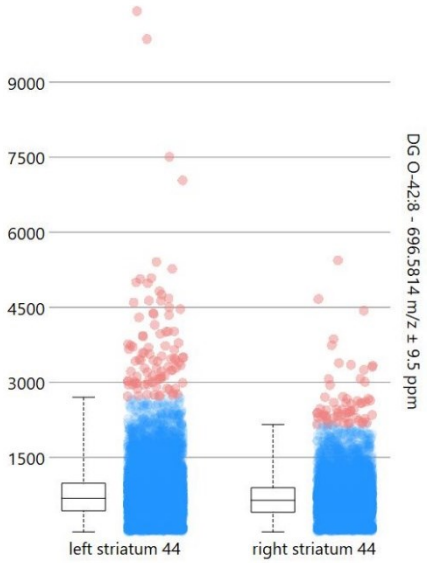

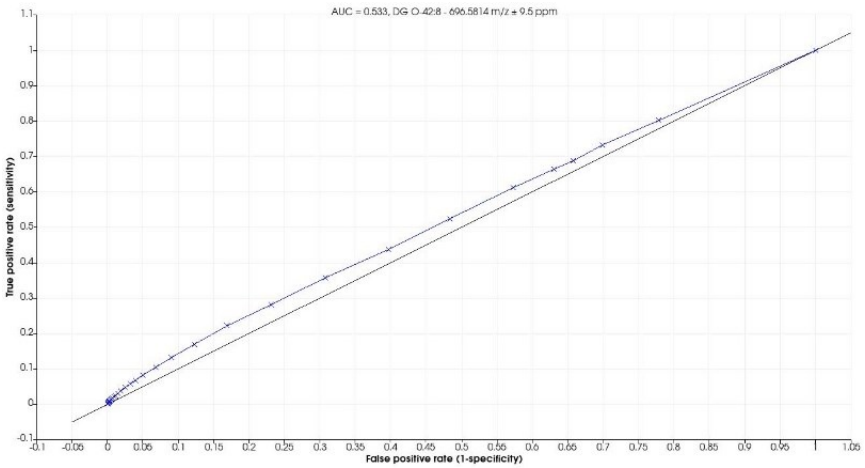

Description of lipid: This lipid approached significance in all lesion vs sham (p = 0.0511) and left lesion vs sham (p = 0.0597), and had strong PCA loading. Likely DG O-42:8, a polyunsaturated diacylglycerol. Its structural similarity to DG O-42:6/7 suggests it participates in shared inflammatory signalling pathways. The high multivariate contribution and near-significance support its relevance to lesion-induced lipid signalling (Podbielska et al., 2021).

5 Discussion

5.1 Lipidomic alterations between lesion and sham groups

This study demonstrates significant lipidomic changes following striatal MS-like induced lesions, particularly phospholipids (PC), sphingolipids, and diacylglycerols (DGs). These changes reflect processes associated with membrane remodelling, neuroinflammation, and oxidative stress, mechanisms relevant in neurodegenerative conditions like multiple sclerosis (MS). Lipidomic analysis revealed significant alterations of specific lipid classes associated with chronic neuroinflammation. Some of which have been previously implicated in MS studies or in neurodegenerative or neuroinflammatory conditions.

Ceramide 36:1 (m/z 588.5311) s for example, a bioactive sphingolipid with a known role in oxidative stress, apoptosis, and pro-inflammatory signalling. Ceramide 36:1 was found to be both near-significantly elevated and contributed to PCA variance. This finding aligns with studies showing ceramide accumulation in both cerebrospinal fluid and MS plaques of MS patients, where it contributes to demyelination and lesion development (Podbielska et al., 2021; Ghorbani & Yong, 2021).

Several phosphatidylcholine (PC) species were altered significantly, suggesting that membrane phospholipid composition and turnover are disrupted in inflamed regions compared to the control slices. The most significant results are of PC O-34:1 (m/z 768.5866) and PC 34:2 (m/z 758.5669), which showed significant alterations between and within hypotheses testing. PCs are central to membrane fluidity and are precursors to pro-inflammatory Lys-phosphatidylcholine (LPC), which is known to increase during demyelination and immune cell infiltration (Cicalini et al., 2019; Ferreira et al., 2020). The targeted list used for this thesis did not contain LPCs, so no conclusions can be drawn. However, based on previous literature, the ion intensities of these lipids would likely have been altered between control and lesioned animals and should be included in future studies (Batista et al, 2019).

Similarly, PE 38:1 (m/z 774.5985, 796.5819) and PE 36:1 (m/z 746.567) were elevated in lesioned tissue, which could reflect glial activation and mitochondrial remodelling, processes known to accompany neuroinflammation (Oliveira-Lima et al., 2019; Razo et al., 2024). Interestingly, although DG species did not reach statistical significance, the high PCA loadings suggest a biologically meaningful role in lesion-associated metabolic shifts. DG O-42:6 (m/z 700.6122) was the strongest contributor to PCA variance (loading = 0.578), despite lacking univariate significance.

This suggests that DG metabolism could be influenced by lesion pathology in ways that vary across individuals or lesion progression states (Johansson et al., 2004).

5.2 Regional lipid shifts in lesioned animals

Distinct regional lipid signatures were also observed within the lesioned animals, particularly when comparing the ipsilateral lesion site to the contralateral striatum. Elevated levels of PE 38:1, PE 36:1, PC 38:6, and PC 40:6 were observed in the ipsilateral striatum compared to the contralateral side. This supports localised membrane remodelling and inflammation.

Cer 36:1 showed both intergroup and regional significance, reinforcing its biological importance. DG species such as DG O-42:6 and DG O-42:7 were again prominent in PCA, despite lacking statistical significance. This variability likely reflects heterogeneity in lesion maturity and immune response (Sjövall et al., 2004).

These findings support the second hypothesis: that lipidomic changes extend beyond the lesioned region, with the contralateral hemisphere also displaying distinct lipid alterations compared to control striata. The presence of inter-hemispheric differences suggests possible compensatory metabolic responses or diffuse inflammatory signalling.

5.3 Multivariate Insights (PCA)

PCA analysis revealed that some lipids with high variance contributions (e.g., DG O-42:6, DG O-42:7) did not reach statistical significance, indicating that univariate tests alone may not fully capture biologically meaningful shifts. This supports the third hypothesis: that multivariate analysis can highlight lipidomic patterns overlooked in conventional statistical testing.

The discrepancy between PCA loadings and Kruskal-Wallis's significance may be due to individual variability in lesion severity or tissue response. Since the sample set included multiple sections from the same animals, the data is linked, suggesting that a repeated-measures approach or mixed-effects modelling might be beneficial in future studies. Additionally, the resolution of MSI data (50 µm for analysis, 20 µm for visualization) provides spatial insights into lipid distribution. Ion images revealed that some lipids, such as Cer 36:1, were concentrated within the lesion core, whereas others (e.g., PCs) were more diffusely distributed. This highlights the value of spatial lipidomics in capturing lesion heterogeneity.

5.4 Methodological considerations

This study has several methodological considerations that may influence interpretation. Firstly, while the Kruskal–Wallis test is appropriate for non-parametric data, it does not account for the linked structure of the dataset of multiple tissue sections derived from the same animal. Future analyses could benefit from statistical approaches such as mixed-effects models or repeated-measures ANOVA to better handle inter-subject variability. Secondly, the lipidomic analysis was limited to a targeted panel of 70 lipids, excluding other relevant classes such as Lys phosphatidylcholines (LPCs), oxidized phospholipids, and bis(monoacylglycerol)phosphates (BMPs), all of which have been linked to neuroinflammation and lesion pathology (Ferreira et al., 2020; Razo et al., 2024; Jain et al., 2020). An untargeted lipidomics approach would provide a broader overview of disease-related lipid alterations.

Usually, the small sample size (six lesioned, three sham mice) would have constrained statistical power and sensitivity to detect lipidomic differences, especially in the presence of biological variability. However many confounding factors such as environment, diet, disease severity are more controlled in an animal study compared to clinical research.

Ion imaging data revealed distinct spatial lipid distributions within lesioned brains, with certain lipids accumulating either centrally in the lesion or more peripherally within the ipsilateral striatum. These patterns underscore the value of region-specific segmentation strategies during analysis. The targeted list showed several significant lipids already, but with a larger sample size, but not significant in hypothesis testing. However, with a larger sample size in future work, detecting anatomical differences is possible.

5.5 Translating lipids to MS

Findings here reflect established patterns in human MS studies, where ceramide accumulation, oxidized phospholipids, and PC metabolism alterations are linked to demyelination and neuroinflammation (Podbielska et al., 2021; Ferreira et al., 2020; Razo et al., 2024). DGs, though underexplored in MS, emerged as strong PCA contributors, suggesting a possible early role in signalling disruptions. Future work should investigate whether DGs act as precursors to inflammatory lipid mediators. Ceramide 36:1 stands out for its PCA and near-statistical relevance. Ceramides drive oxidative stress, inflammatory cascades, and programmed cell death. Modulating

ceramide synthesis or downstream enzymes like ceramidase or sphingosine kinase may offer therapeutic benefits (Podbielska et al., 2021; Ghorbani & Yong, 2021; Razo et al., 2024; Bazan, 2005). Altered levels of PEs and PCs may reflect glial reactivity or early apoptotic processes (Ferreira et al., 2020; Dickens et al., 2017). Similar phospholipid disturbances have been observed in MS tissue and animal models (Oliveira-Lima et al., 2019).

5.6 Lipid biomarkers and therapeutic Implications

Among the lipid alterations identified, the elevation of ceramide 36:1 (m/z 588.5311) in lesioned tissue stands out for both its statistical significance and its mechanistic implications. Ceramides are well-established mediators of neuroinflammatory signalling, oxidative stress, and programmed cell death. Thus, Ceramides make for compelling targets for therapeutic intervention in multiple sclerosis and related neurodegenerative conditions (Podbielska et al., 2021; Ghorbani & Yong, 2021; Razo et al., 2024; Bazan, 2005). Pharmacological modulation of ceramide synthesis or downstream signalling, such as via ceramidase or sphingosine kinase pathways, may offer opportunities to mitigate inflammatory damage and promote tissue preservation (Bazan, 2005; Ferreira et al., 2020).

Alterations in phosphatidylethanolamines (PE 36:1, PE 38:1) and phosphatidylcholines (PC O-34:1, PC 34:2) further suggest dynamic changes in membrane architecture, glial reactivity, and early apoptotic remodelling (Ferreira et al., 2020; Bazan, 2005; Dickens et al., 2017). Similar phospholipid disruptions have also been observed in human MS lesions and experimental autoimmune encephalomyelitis (EAE) models (Oliveira-Lima et al., 2019).

Notably, the lipid annotations in this study were derived from software-based database matching, and while accurate to the level of m/z and molecular formula, it may not unambiguously distinguish isomeric species. Though m/z alignment supports identification, definitive structural validation via MS/MS or co-elution with standards remains an important step for future studies to ensure molecular specificity.

5.7 Future Directions in Clinical Lipidomics

Despite growing evidence that lipid dysregulation plays a central role in neuroinflammation and neurodegeneration, challenges remain in fully understanding lipid-mediated mechanisms in MS. Current targeted panels, while informative, risk overlooking key lipid species such as bis(monoacylglycerol)phosphates (BMPs), N-acyl phosphatidylethanolamines (NAPEs), and

oxidized phospholipids, all of which have been linked to microglial activation, oxidative stress, and mitochondrial dysfunction (Jain et al., 2020; Razo et al., 2024; Ferreira et al., 2020). Despite this, impressively significant lipidomic results have provided evidence of known neuroinflammatory biomarkers and some yet unsupported by available literature. This implies the current research is in line with the field and has contributed to what is known from lipidomic implications in MS and neuroinflammation. Future research can definitely follow up on these new findings.

Future research should also focus on an untargeted lipidomic approach to discover lipid changes beyond those currently discussed, while combining lipid data with imaging techniques like PET or MRI to capture the diversity of MS lesions (Razo et al., 2024). Sampling regions like the lesion core, surrounding tissue, and opposite hemisphere will enhance spatial specificity and help us understand how lipid metabolism responds locally and brain-wide to neuroinflammation (Mallah et al., 2019; Rebelo et al., 2021). Connecting these patterns to lesion severity or immune cell presence could improve biological interpretation. Long-term studies and functional assays will be essential to examine early versus late-stage lipid changes in MS.

References

Anthony, D., Couch, Y., Losey, P., & Evans, M. (2012). The systemic response to brain injury and disease. *Brain, Behavior, and Immunity*, 26, 534-540. https://doi.org/10.1016/j.bbi.2011.10.011.Batista, C., Gomes, G., Candelario-Jalil, E., Fiebich, B., & De Oliveira, A. (2019). Lipopolysaccharide-Induced Neuroinflammation as a Bridge to Understand Neurodegeneration. International Journal of Molecular Sciences, 20. https://doi.org/10.3390/ijms20092293.

Bazan, N. (2005). Lipid signaling in neural plasticity, brain repair, and neuroprotection. Molecular Neurobiology, 32, 89-103. https://doi.org/10.1385/MN:32:1:089.

Belloli, S., Zanotti, L., Murtaj, V., Mazzon, C., Di Grigoli, G., Monterisi, C., Moresco, R. (2018). 18F-VC701-PET and MRI in the in vivo neuroinflammation assessment of a mouse model of multiple sclerosis. Journal of Neuroinflammation, 15. https://doi.org/10.1186/s12974-017-1044-x.

Bowman, A., Heeren, R., & Ellis, S. (2019). Advances in mass spectrometry imaging enabling observation of localised lipid biochemistry within tissues. TrAC Trends in Analytical Chemistry. https://doi.org/10.1016/J.TRAC.2018.07.012.

Bruker Daltonics. (2025). MALDI TimsTOF fleX mass spectrometer [Mass spectrometer]. Bruker Daltonics.

Del Boccio, P., Pieragostino, D., Di Ioia, M., Petrucci, F., Lugaresi, A., De Luca, G., Gambi, D., Onofrj, M., Di Ilio, C., Sacchetta, P., & Urbani, A. (2011). Lipidomic investigations for the characterization of circulating serum lipids in multiple sclerosis. Journal of proteomics, 74 12, 2826-36. https://doi.org/10.1016/j.jprot.2011.06.023.

Difco Laboratories. (n.d.). Difco H37Ra Mycobacterium tuberculosis [Bacterial strain, BD UK]. Becton, Dickinson and Company.

DiSabato, D., Quan, N., & Godbout, J. (2016). Neuroinflammation: the devil is in the details. Journal of Neurochemistry, 139. https://doi.org/10.1111/jnc.13607.

Dickens, A., Tovar-Y-Romo, L., Yoo, S., Trout, A., Bae, M., Kanmogne, M., ... & Haughey, N. (2017). Astrocyte-shed extracellular vesicles regulate the peripheral leukocyte response to inflammatory brain lesions. Science Signaling, 10. https://doi.org/10.1126/scisignal.aai7696.

Fernández, R., Garate, J., Martín-Saiz, L., Galetich, I., & Fernández, J. (2018). Matrix Sublimation Device for MALDI Mass Spectrometry Imaging. Analytical Chemistry, 91(1), 803-807. https://doi.org/10.1021/acs.analchem.8b04765.

Fernández-Beltrán, L., Godoy-Corchuelo, J., Losa-Fontangordo, M., Williams, D., Matías-Guiu, J., & Corrochano, S. (2021). A Transcriptomic Meta-Analysis Shows Lipid Metabolism Dysregulation as an Early Pathological Mechanism in the Spinal Cord of SOD1 Mice. International Journal of Molecular Sciences, 22. https://doi.org/10.3390/ijms22179553.

Ghorbani, S., & Yong, V. (2021). The extracellular matrix as modifier of neuroinflammation and remyelination in multiple sclerosis.. *Brain : a journal of neurology*. https://doi.org/10.1093/brain/awab059.

Ferreira, H., Neves, B., Guerra, I., Moreira, A., Melo, T., Paiva, A., & Domingues, M. (2020). An overview of lipidomic analysis in different human matrices of multiple sclerosis. Multiple Sclerosis and Related Disorders, 44, 102189. https://doi.org/10.1016/j.msard.2020.102189.

Hansen, S., & Wang, H. (2023). The shared role of cholesterol in neuronal and peripheral inflammation. Pharmacology & Therapeutics, 108486. https://doi.org/10.1016/j.pharmthera.2023.108486.

Hasselmann, J., Karim, H., Khalaj, A., Ghosh, S., & Tiwari-Woodruff, S. (2017). Consistent induction of chronic experimental autoimmune encephalomyelitis in C57BL/6 mice for the longitudinal study of pathology and repair. Journal of Neuroscience Methods, 284, 71-84. https://doi.org/10.1016/j.jneumeth.2017.04.003.

Innovagen. (2025). Myelin oligodendrocyte glycoprotein (MOG35–55) peptide [Peptide reagent]. Innovagen AB.

Jain, P., Chaney, A., Carlson, M., Jackson, I., Rao, A., & James, M. (2020). Neuroinflammation PET Imaging: Current Opinion and Future Directions. The Journal of Nuclear Medicine, 61, 1107-1112. https://doi.org/10.2967/jnumed.119.229443.

Kalkowski L, Golubczyk D, Kwiatkowska J, Domzalska M, Walczak P, Malysz-Cymborska I (2022) Local autoimmune encephalomyelitis model in a rat brain with precise control over lesion placement. PLoS ONE 17(1): e0262677. https://doi.org/10.1371/journal.pone.0262677

Mallah, K., Quanico, J., Raffo-Romero, A., Cardon, T., Aboulouard, S., Devos, D., Kobeissy, F., Zibara, K., Salzet, M., & Fournier, I. (2019). MALDI MSI of Lipids in Experimental Model of Traumatic Brain Injury Detects Acylcarnitines as Injury Related Markers.. *Analytical chemistry*. https://doi.org/10.1021/acs.analchem.9b02633.

Mallah, K., Quanico, J., Trede, D., Kobeissy, F., Zibara, K., Salzet, M., & Fournier, I. (2018). Lipid Changes Associated with Traumatic Brain Injury Revealed by 3D MALDI-MSI. Analytical Chemistry, 90(17), 10568-10576. https://doi.org/10.1021/acs.analchem.8b02682.

Mi, Y., Qi, G., Vitali, F., Shang, Y., Raikes, A., Wang, T., Jin, Y., Brinton, R., Gu, H., & Yin, F. (2023). Loss of fatty acid degradation by astrocytic mitochondria triggers neuroinflammation and neurodegeneration. *Nature Metabolism*, 5, 445-465. https://doi.org/10.1038/s42255-023-00756-4.

Momchilova, A., Pankov, R., Alexandrov, A., Markovska, T., Pankov, S., Krastev, P., ... & Pinkas, A. (2022). Sphingolipid Catabolism and Glycerophospholipid Levels Are Altered in Erythrocytes and Plasma from Multiple Sclerosis Patients. International Journal of Molecular Sciences, 23. https://doi.org/10.3390/ijms23147592.

Oliveira-Lima, O., Carvalho-Tavares, J., Rodrigues, M., Gomez, M., Oliveira, A., Resende, R., ... & Pinto, M. (2019). Lipid dynamics in LPS-induced neuroinflammation by DESI-MS imaging. Brain, Behavior, and Immunity, 79, 186-194. https://doi.org/10.1016/j.bbi.2019.01.029.

Podbielska, M., Szulc, Z., Ariga, T., Pokryszko-Dragan, A., Fortuna, W., Bilińska, M., ... & Hogan, E. L. (2020). Distinctive sphingolipid patterns in chronic multiple sclerosis lesions. Journal of Lipid Research, 61, 1464-1479. https://doi.org/10.1194/jlr.RA120001022.

Ransohoff, R., Kivisäkk, P., & Kidd, G. (2003). Three or more routes for leukocyte migration into the central nervous system. Nature Reviews Immunology, 3, 569-581. https://doi.org/10.1038/nri

Razo, I., Shea, K., Allen, T., Boutin, H., McMahon, A., Lockyer, N., & Hart, P. R. (2024). Accumulation of Bioactive Lipid Species in LPS-Induced Neuroinflammation Models Analysed with Multi-Modal Mass Spectrometry Imaging. International Journal of Molecular Sciences, 25. https://doi.org/10.3390/ijms252212032.

Rebelo, A. L., Gubinelli, F., Roost, P., Jan, C., Brouillet, E., Van Camp, N., & Pandit, A. (2021). Complete spatial characterisation of N-glycosylation upon striatal neuroinflammation in the rodent brain. Journal of Neuroinflammation, 18. https://doi.org/10.1186/s12974-021-02163-6.

SCiLS™ Lab. (2025). SCiLS Lab software (Version 2025a Pro) [Computer software]. Bruker Daltonics

Sjövall, P., Lausmaa, J., & Johansson, B. (2004). Mass spectrometric imaging of lipids in brain tissue. Analytical Chemistry, 76(15), 4271–4278. https://doi.org/10.1021/AC049389P.

Stoelting Co. (2025). Stereotaxic frame [Laboratory equipment]. Stoelting Co.The Hong Kong Polytechnic University, UCEA. (2025, July 8).

Bruker timsTOF Pro 2 Mass Spectrometer [Image]. UCEA Equipment and Facility. The Hong Kong Polytechnic University. https://www.polyu.edu.hk/ucea/equipment-and-facility/equipment/timstof-ms/

Trim, P. J., Atkinson, S. J., Princivalle, A. P., Marshall, P. S., West, A., & Clench, M. R. (2008). Matrix-assisted laser desorption/ionisation mass spectrometry imaging of lipids in rat brain tissue with integrated unsupervised and supervised multivariant statistical analysis. Rapid

Communications in Mass Spectrometry, 22(10), 1503–1509. https://doi.org/10.1002/rcm.3498.

Turku Center for Disease Modeling. (2024). Laboratory Animal Welfare Course. University of Turku. https://www.tcdm.fi/education/laboratory-animal-welfare-course/

Voskuhl, R. R., & MacKenzie-Graham, A. (2022). Chronic experimental autoimmune encephalomyelitis is an excellent model to study neuroaxonal degeneration in multiple sclerosis. Frontiers in Molecular Neuroscience, 15, 1024058. https://doi.org/10.3389/fnmol.2022.1024058.

Wilcockson, D. C., Campbell, S. J., Anthony, D. C., & Perry, V. H. (2002). The systemic and local acute phase response following acute brain injury. Journal of Cerebral Blood Flow & Metabolism, 22(3), 318–326. https://doi.org/10.1097/00004647-200203000-00009.

Yoon, J., Seo, Y., Jo, Y., Lee, S., Cho, E., Cazenave-Gassiot, A., Suh, P.-G. (2022). Brain lipidomics: From functional landscape to clinical significance. Science Advances, 8(51), eadc9317. https://doi.org/10.1126/sciadv.adc9317.